

# Trends in Biorobotic Autonomous Undersea Vehicles

Promode R. Bandyopadhyay

**Abstract**—The emergence of biorobotic autonomous undersea vehicle (AUV) as a focus for discipline-integrated research in the context of underwater propulsion and maneuvering is considered within the confines of the Biorobotics Program in the Office of Naval Research. The significant advances in three disciplines, namely the biology-inspired high-lift unsteady hydrodynamics, artificial muscle technology and neuroscience-based control, are discussed in an effort to integrate them into viable products. The understanding of the mechanisms of delayed stall, molecular design of artificial muscles and the neural approaches to the actuation of control surfaces is reviewed in the context of devices based on the pectoral fins of fish, while remaining focused on their integrated implementation in biorobotic AUVs. A mechanistic understanding of the balance between cruising and maneuvering in swimming animals and undersea vehicles is given. All aquatic platforms, in both nature and engineering, except during short duration burst speeds that are observed in a few species, appear to lie within the condition where their natural period of oscillation equals the time taken by them to travel the distance of their own lengths. Progress in the development of small underwater experimental biorobotic vehicles is considered where the three aforementioned disciplines are integrated into one novel maneuvering device or propulsor. The potential in maneuvering and silencing is discussed.

**Index Terms**—Artificial muscles, autonomous undersea vehicles (AUVs), biorobotics, fish biology, high-lift, hydrodynamics, internal Froude number, maneuvering, neuroscience-based control, pectoral fins, polymers.

## I. INTRODUCTION

ENGINEERS have been implementing a set of principles of locomotion to build swimming and flying platforms for some time. This effort has led to matured designs of submarines and autonomous undersea vehicles (AUVs). There are some “unused” principles that are risky to implement. However, recent interest in swimming and flying animals show that these “risky principles” are routinely used and are indeed feasible in a system. Specifically, steady-state hydrodynamics, on which submarines and aircraft are designed, do not explain the hovering or rapid turning of coral reef fish or the high lift of fruit flies. In animal swimming and flying, unsteady hydrodynamics is the norm. Engineers are yet to build vehicles based on these unsteady high-lift principles. Because of cost and reliability concerns, conventional motor drives are not capable of producing the dynamic three-dimensional (3-D) motions of these lifting surfaces. Anisotropic artificial muscles (AM) that have properties akin to those of mammalian muscles are

needed. Thus, to spark the next revolution in low-speed maneuvering, silencing, signature reduction, and power or weight reduction in underwater or aerial platforms, the integration of the science and technology of high-lift biohydrodynamics and artificial muscle is needed. The combination then becomes amenable to neuroscience-based control—allowing a vehicle to be autonomous (that is, characteristics such as adaptability and nonlinear controllability) in its underwater or aerial surrounding—or for an underwater weapon to have unprecedented stealth. Stated in another way, the implementation of the “unused principles” could be feasible if the approach is bio-inspired and multidisciplinary. The Biorobotics Program within the Office of Naval Research (ONR) is attempting to develop the underlying science and technology. Benchmarks are being prepared from the conceptual design of a biorobotic AUV with advanced dolphin-like mobility.

The spectrum from science to technology required for the development of biorobotic AUVs is as follows in order of maturity. The first area involves the understanding of fish pectoral fin muscle physiology and their neuroscience-based control mechanism. The second area concerns the molecular design of conducting electro-active polymers and other competitive AMs to match or exceed the properties of mammalian muscles, optimization of the conflicting material properties for use in underwater vehicles, and the production and basic engineering of such muscles. The required material properties are a compact, small-volume actuator with optimum combination across the entire matrix of strain, stress, power, efficiency and weight; use as an actuator, power source or sensor; amenability to neural net structures; and overall, closeness to biology in key performance measures. The third area focuses on the engineering implementation of the anisotropic physiology and neuroscience-based control of platform motion, particularly of fish-like pectoral fins via AM whose deflections are coded on a microprocessor. The fourth area concerns the scaled study of high-lift mechanism of flexible 3-D pectoral fins, which are AUV-appropriate aquatic animals that are undergoing the motions of heave, pitch, and twist, as well as Reynolds number scaling laws. The fifth area covers the ocean engineering extension of the high-lift mechanism to high Reynolds numbers in rigid cylindrical hulls. The sixth area describes the system-based integration of the distilled sciences of the three disciplines into a pectoral fin-like control surface for rigid hull forms [1]. This integration would produce a programmable and lightweight control surface allowing underwater hovering and precision maneuvering. It is essential that the diverse disciplines be integrated early to develop one single viable product. This approach builds on the biorobotic research conducted at the Naval Undersea Warfare Center (NUWC), Newport, RI, which has been reviewed elsewhere [1], [2], and was the focus of a pre-workshop [3].

Manuscript received December 6, 2002; accepted July 7, 2004. This work was supported by the Office of Naval Research. Associate Editor: J. Lynch.

The author was with the Office of Naval Research, Arlington, VA 22217 USA. He is now with the Naval Undersea Warfare Center, Newport, RI 02841 USA (e-mail: BandyopadhyayPR@Npt.NUWC.Navy.Mil).

Digital Object Identifier 10.1109/JOE.2005.843748

The aforementioned areas in the spectrum of science and technology are arranged in this paper in the following order. In Section II, these topics are presented to describe the background: contemporary engineering AUVs and performance needs, summary of lessons from research on biology-inspired platforms and historical trends, and a mechanistic framework for the measurement of maneuverability which is gaining increasing importance compared to cruising. Section III gives the scientific hydrodynamic foundation and the topics covered are: mechanism of high-lift, engineering devices and feasibility. In Section IV, artificial muscle actuator technology is reviewed and its feasibility is explored in the present context. In Section V, advances in neuro-science based control is distilled to determine how a controller for a small underwater vehicle could be built. In Section VI, we examine the feasibility of integrating the disciplines of hydrodynamics, artificial muscle technology and neuro-science based control in to AUVs. In Section VII, several contemporary biorobotic AUVs are compared with the above-mentioned concept of integrated AUV. In Section VIII, the potential impact of this conceptual discipline integrated biorobotic AUV on radiated noise is explored. Concluding remarks on trends are made in Section IX. Mechanism-based simulation, analytical modeling, novel experimentation, and design are discussed.

## II. BACKGROUND: TECHNOLOGY AND SCIENCE

### A. Contemporary Engineering AUVs

The three services are developing unmanned vehicles for both surveillance and combat. Although endurance is the early focus, mission success depends on low-speed maneuverability. Swimming animals excel in this capability. Consequently, if successful, the actuators from this Program would affect several Department of Defense (DOD) Programs. In the littoral zone, the Navy would be impacted in the areas of low-speed maneuverability in the smaller platforms of AUV, countermeasures (CM), and Gliders in the short to medium timeframe, and in the stealth of weapons in the longer timeframe. AUVs, rather than making high-resolution, one-dimensional (1-D) linear scans for mine detection, would hover, encircle, and diagnose objects to improve sensor competence and gauge heights of obstacles for avoidance. Energy and communication bandwidth of AUVs would be impacted. AM would make long-duration underwater gliders maneuverable. Integrated AM, high lift, and their neuroscience-based control would make submarine-launched CMs mobile and their clustering feasible. Because vibration from motors that drive propulsors and control surfaces is transmitted to the hull and is the main source of noise radiated from vehicles, the elimination of motors by conducting polymer AM would lower hull vibration, thereby causing unprecedented platform quieting.

The history of AUV development from a systems point of view has been reviewed recently [4]. All AUVs, because of their similarity in size and motion to larger aquatic animals, are candidates for biorobotic improvements. A wide variety of about 240 contemporary AUVs exist. The IEEE JOURNAL OF OCEANIC ENGINEERING [5], in a special issue, presents a scientific description of some of them. These platforms are char-

acterized by a rigid and cylindrical small hull form and are based on well-established design principles. Of these, Fig. 1 shows the SLOCUM Glider and Fig. 2 shows the REMUS AUV. The REMUS has an axis-aligned propeller thrust, whereas the Ranger MicroAUV has a hinge that allows thrust vectoring. CETUS II has a rigid Manta-like hull with two off-axis propellers, which is another means of thrust vectoring. The latter two can be seen as conventional engineering retrofits to fill a perceived gap in maneuverability in the REMUS.

Fig. 3 shows an underwater CM with a small propulsor for limited mobility, which is also a candidate for biorobotic improvement. These platforms are small, about 2–3 m in length, are lightweight whereby they can be handled manually, and they mostly operate at low speeds of a few knots and higher. They are seen as platforms for carrying arrays of sensors for hydrographic, or for minefield surveys, submarine CMs, or for underwater installation surveys. These platforms are the current targets for biorobotic performance enhancement.

An aquatic animal could be considered the perfect autonomous undersea platform that is optimized for a specific habitat, which is the business of survival and procreation in a certain environment. This model, namely aquatic animal, is not an idealized hypothetical platform, but one that is winning the competition of survival. Thus, feasibility of the full system is not in doubt. The issue is bridging the gap in science and technology between nature and engineering in specific disciplines.

In the AUV context, the question is raised regarding the differences between relevant aquatic animals and conventional AUVs. Biosensors and their signal processing are considered elsewhere [6]. Only a small part of the DARPA Program [7] related to the flight of fruit flies is included and only the motion-related issues of the platform are of interest. Low-speed, precision maneuvering ability in aquatic animals is an example of the differences, which can be broadly defined by several characteristics. The first difference is its hovering ability produced by pectoral fins or hull forms, which is circulation generation in the absence of a forward speed. The next difference involves short radius turning that is executed by a phased neurally controlled operation of one fin or a set of circulation fins. This motion can also be sudden acceleration or burst speed and deceleration in response to predator-prey dynamics, which is poorly understood and involves neural control of sets of muscles. Finally, this ability can also be a combination of deceleration, followed by short radius turning and acceleration, resulting in obstacle avoidance, such as saccades of flies. These maneuvering motions can be accomplished primarily by flexible dynamic pectoral fins, which will be discussed later. The various circulation control surfaces (Fig. 4) cycle their pitch, heave, and twist in a phased manner, and are flexible. These abilities seem amenable to engineering by pectoral fins built of AMs and their neuroscience-based control. These aspects will be briefly discussed. Finally, the differences in power plant and the requirement for stealth dictate that ideally the motor shaft gear drive trains in undersea vehicles need to be supplanted by conducting AMs to reduce hull vibration and make more room available for payloads.

Fig. 5 shows a hypothetical order of magnitude growth in the global market of AUVs that could be a target for biorobotic improvement. The assumptions are current units in  $10^2$  s, cost

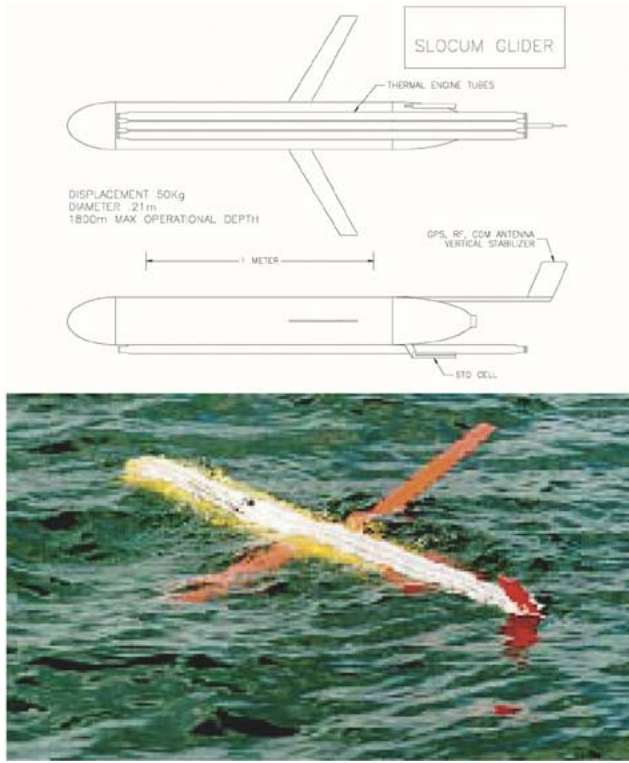


Fig. 1. Gliders are small, lightweight, and low-speed vehicles.



Fig. 2. AUVs are small lightweight and low-speed vehicles.

in \$10<sup>2</sup> sK, and a growth rate of 10% in units and cost. In a decade, there can be an increase to thousands of units, each with increasing gross weight and cost rising to \$M per unit, and the overall market rising to \$B. Biorobotic AUVs would thus seem to have an impact potential.

#### B. Bioengineering Lessons From ONR Biorobotics Program

The Program covers a range of platform scales. The biological models encompass fruit flies ( $O(1\text{ mm})$ ), cockroaches ( $O(10\text{ mm})$ ), and guppy fish ( $O(100\text{ mm})$ ), whereas their robotic counterparts range, from MFI, the Micro-flying Insect ( $O(10\text{ mm})$ ), the Sprawlita ( $O(100\text{ mm})$ ), and the NUWC multidegree of freedom, full-scale maneuvering foil ( $O(1000\text{ mm})$ ), respectively.



Fig. 3. CMs are generally small, lightweight, and nearly immobile vehicles. A more contemporary slightly mobile version with a close-up of the hovering system is shown in the lower picture.

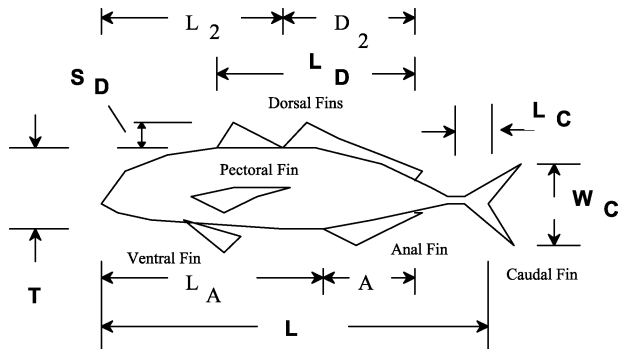


Fig. 4. Typical fin control surfaces and morphological length scales of a fish [54].

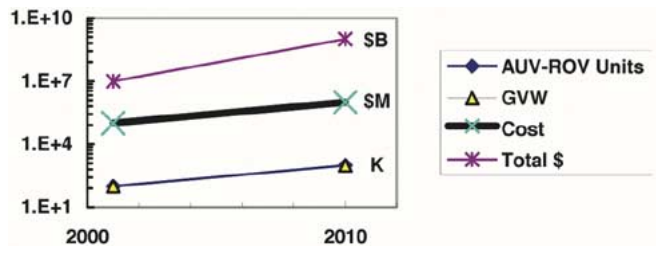


Fig. 5. Projected commercial market deemed as target of biorobotic AUVs.

In the development of these platforms, the question was raised regarding what was learned from biology that conventional engineering did not know. Based on the experience of walking and flying biorobots known as Sprawlita [8] and MFI [9], Tables I and II present some answers. They involve the implementation of new mechanisms that are not widely used in engineering, such as structural compliance or high-lift aerodynamics, giving new performance capabilities; approaches to platform motion control, namely building layers of active control over a basic layer of passive control offering robustness; fewer sensors; and a lower cost to build and operate.

TABLE I  
KEY IDEAS FROM COCKROACH-BASED BIOLOGY TO BIOMIMETIC ROBOTS LIKE SPRAWLITA [8]

| Biology   | <i>Sprawlita</i> : Bio-engineering  | Conventional Engineering  |
|---|---|---|
| Passive mechanical <b>compliance</b> (inverse of stiffness) and <b>damping</b> (energy dissipation) in insect joints promote stable running with open-loop control.<br>Numerical models of insects confirm the predicted stabilizing effects [10].  | Legs have <b>custom-tuned flexures</b> that bend with compliance and damping, resulting in stable running with open-loop control. Documented similarity of motions and ground-reaction forces to those measured in insect running [11].<br><br>Price: \$100 for SDM (Shape Deposition Manufacturing) legs<br>Power: 9 W to run at 6 body-lengths/second.<br>Life: millions of cycles without failure<br><br><i>Lessons:</i> how to specify and create compliant legs for stability + speed.   | Little passive compliance and damping. Stability achieved through <b>high-bandwidth servoing</b> , with expensive velocity sensors, amplifiers, microprocessor, and a high “cost of control” added to the energy required for propulsion.<br><br>Price: \$5000 for leg feedback systems<br><br>Power: 14 W to run at 6 body-lengths/second.<br>Life: estimated mean-time between failures (MTBF) of 30 minutes for prototypes.  |
| Animals run at resonance, with the spring loaded inverted pendulum ( <b>SLIP</b> ) model as a “template.” In insects this is achieved using active thrusting along legs and mostly passive rotation at hips [12]. Result is efficient, stable oscillation in response to open-loop feed-forward activation from Central Pattern Generator (CPG).  | Propulsion by active thrusting + passive hip flexures. Fast, stable running at <b>resonance</b> with open-loop valve activation pattern.<br>No sensing, actuation or control cost for hips. SLIP-like force, motion pattern confirmed in tests [12].<br><br>Price, Power (see above)<br><br><i>Lessons:</i> which parameters (stride period, leg angles, and compliance) are most important and which degrees of freedom should be active or passive.   | Leg actuation requires servos for each degree of freedom. State-based control requires expensive sensors, actuators and controllers for each degree of freedom. Typical cost and complexity increase at least as $N^2$ for N degrees of freedom.<br><br>Price, Power (see above)  |
| Sensory response is <b>layered</b> on top of passively stable system + feed-forward (CPG) pattern [13, 14]. This approach gives ability to adapt to changing conditions while retaining speed and robustness, because the low-level “preflexes” are always present. Sensors are numerous, have high dynamic range, are highly non-linear and cross-coupled. New results on insect perturbation response, measured on running insects, show sensor-based adaptation over multiple strides. | Implemented adaptation strategies, are <b>layered</b> on top of passively stable system. If conditions deviate from expectations used in creating the adaptation strategies, the system reverts to baseline stable behavior. The adaptation strategies use only <b>simple non-linear sensors</b> [15].<br><br>Price: \$200 for inexpensive sensors and small microprocessor.<br>Energy cost: (sensor, microprocessor): 0.3 W.<br><br>Performance: up to 4x faster running with adaptation as conditions change.<br><i>Lessons:</i> Theoretical dynamics and control arguments can be made to support the biological observations. | Complex control system with multiple layers. Adaptation software is built on top of low-level servo software for controlling the limbs and maintaining stability.<br>Expensive high-power microprocessor and high-quality, linear sensors required. Result is not robust (behaves poorly when conditions get outside anticipated range for which the controller was tuned).<br>Price: \$5000 for expensive sensors and microprocessor.<br>Energy cost for adaptation (sensors, microprocessor): 2 W.<br>Performance: unknown (not demonstrated in conventional approach). |
| Compliant sensorized appendages (e.g. grippers, antennae) automatically <b>conform</b> to surfaces without high-level control and provide rich array of contact information [16, 17].   | Compliant gripper fingers close on objects without active control. Sensors are embedded using SDM (Shape Deposition Manufacturing). Open-space positioning is poorer than with conventional servoing but force regulation is superior and actuator requirements are reduced.<br>Price: \$100 materials, \$200 sensors.<br>energy cost: 0.4 W, peak  | Stiff parallel-jaw grippers with load cells. Accurate position and force control achieved through high-bandwidth servoing. Contact instabilities are always a danger. Force sensors are fragile and frequently need to be recalibrated.<br><br>Price: \$3000 for processing power, sensors, servo.<br>energy cost: 1.0 W, peak  |
| <b>Gecko foot adhesion: Van der Waals forces</b> proven as the underlying mechanism, in combination with very large surface area obtained by recursive setae structures [18].   | Ongoing work at Berkeley in collaboration with R. Fearing to create synthetic setae. First generation is on a flat surface. Second generation may be embedded into 3D compliant feet using SDM.   | Nothing comparable exists.<br><br>Sticky adhesive alternatives have many disadvantages.   |

### C. Dolphin Biosonar and Biorobotic AUV

An important function of AUVs is mine detection. The benchmark of false alarm in detection is set by the U.S. Navy Marine Mammal Systems in which levels achieved by dolphins [6] play a role. The AUV development for this task may be seen as an effort to replace the human-in-the-loop, namely the

diver, and execute the task via automation with equal or reduced false-alarm rates. This determines the goal of the Biorobotics Program, namely bridging the gap between nature and engineering by improving the performance of the latter as compared with the former. This gap in maneuverability will be partially quantified later and the scientific foundation for the scheme for bridging the gap will be presented. This is the general aim of

**TABLE II**  
**KEY IDEAS FROM FRUIT-FLY BASED BIOLOGY TO BIOMIMETIC ROBOT CALLED MICRO-FLYING INSECT [9]**

| Biology  | MFI Implementation   | Conventional Engineering  |
|--|--|---|
| <i>1. Actuation:</i><br>Mechanically resonant fly muscle/wing system runs with no inertial cost, no rotary bearings [19].  | The MFI uses custom piezo unimorph actuators which run at resonance with wing inertia. Internal losses are very low.<br><br><i>Lessons:</i> High power resonant systems can be built by combining a mechanical amplifying stage with small displacement, high force actuators [20-22].   | DC motor, using high RPM to get high power density, and a gear box leading to high friction losses and difficulty in scaling. Smallest motor (Faulhaber) has mass of 70 mg without a gear box, very difficult to scale down to insect size. High power losses in accelerating/decelerating of inertial load such as wing.       |
| <i>2. Aerodynamics:</i><br>The mechanisms of high lift forces from flapping insect flight were identified [23, 24] as due to rotational lift combined with wake capture and delayed stall; they allow insects to lift twice their body mass. | The MFI thorax was designed to achieve 120 deg stroke, 90 deg rotation at 150 Hz, based on these biological insights [20, 25].<br><br><i>Lessons:</i> Wing rotation timing can be used to control lift and thrust forces, as well as pitch and roll moments.   | At blowfly size and smaller, fixed angle of attack propellers require twice the power for the same lift forces due to increased drag losses. Beating wings which can not control rotation timing would not be able to precisely control flight forces for stability.  |
| <i>3. Wing Kinematics:</i><br>The insect wing hinge uses 20 steering muscles with a very sophisticated cam arrangement [26].   | The MFI thorax uses a spherical 5 bar as a wing differential and is driven with just 2 actuators [27, 28, 37].<br><br><i>Lessons:</i> How to make lightweight kinematic elements using flexures instead of pin joints.   | A conventional differential mechanism uses gears, which would be very heavy, require watchmaker tolerances, and have higher losses than the flexural differential.  |
| <i>4. Sensors:</i><br>The fly uses a tightly coupled system with optic flow sensors for obstacle detection/avoidance [28] and halteres for pitch/roll/yaw velocity. Ocelli sensors provide pitch and roll angles.                            | Prototype haltere and ocelli sensors were fabricated and tested in simulation [29-32].<br><br><i>Lessons:</i> Simple biomimetic sensors in combination can stabilize the flight of the MFI and give rise to useful behaviors without requiring sophisticated reasoning or signal processing systems.   | A conventional approach would use MEMS sensors, which require too much power, lack the dynamic range of the haltere, and would be difficult to synchronize with the MFI wing beat. Due to the inertia forces of the wings, it would be difficult to detect small angular accelerations using a conventional MEMS accelerometer. |
| <i>5. Flight Control:</i><br>The fly flight control system allows flies to robustly track odor plumes, defend territory, and find food sources using a relatively simple suite of sensors and strategies [28].                               | In simulation, we have shown how a biomimetic haltere-like gyro combined with an optical flow sensor can be used to stably hover, and recover the MFI from an inverted position [32, 34, 35, 36].<br><br><i>Lessons:</i> By updating desired flight forces and moments at every wing stroke, a simple discrete time control system gives good performance in simulation. We conjecture that the fly is also performing a wing-stroke by wing-stroke update of desired wing rotation timing and trajectory. | A conventional approach would have developed a sophisticated non-linear controller taking into account all aerodynamics, wing dynamics, etc. This controller would be very sensitive to design parameters and require an excess amount of computation to fit on the MFI.  |
| <i>6. Structure and Joints:</i><br>Insects use flexural joints and exoskeleton links made from resilin and chitin.   | The MFI thorax is fabricated using polyester joints and exoskeleton links made with carbon fiber sheets with a carbon fiber core.<br><br><i>Lessons:</i> Inspired by insects, we have developed a rapid prototyping process which allows us to create high performance millimeter scale electromechanical systems with high strength-to-weight ratio ( $10X$ silicon), low inertia, low dissipation, and multiple joints [22, 33].   | A conventional approach would use either silicon MEMS with a 3 month lead time between versions, or expensive precision watch making technology. Neither is capable of the 150 Hz wing flapping frequency needed by MFI.  |

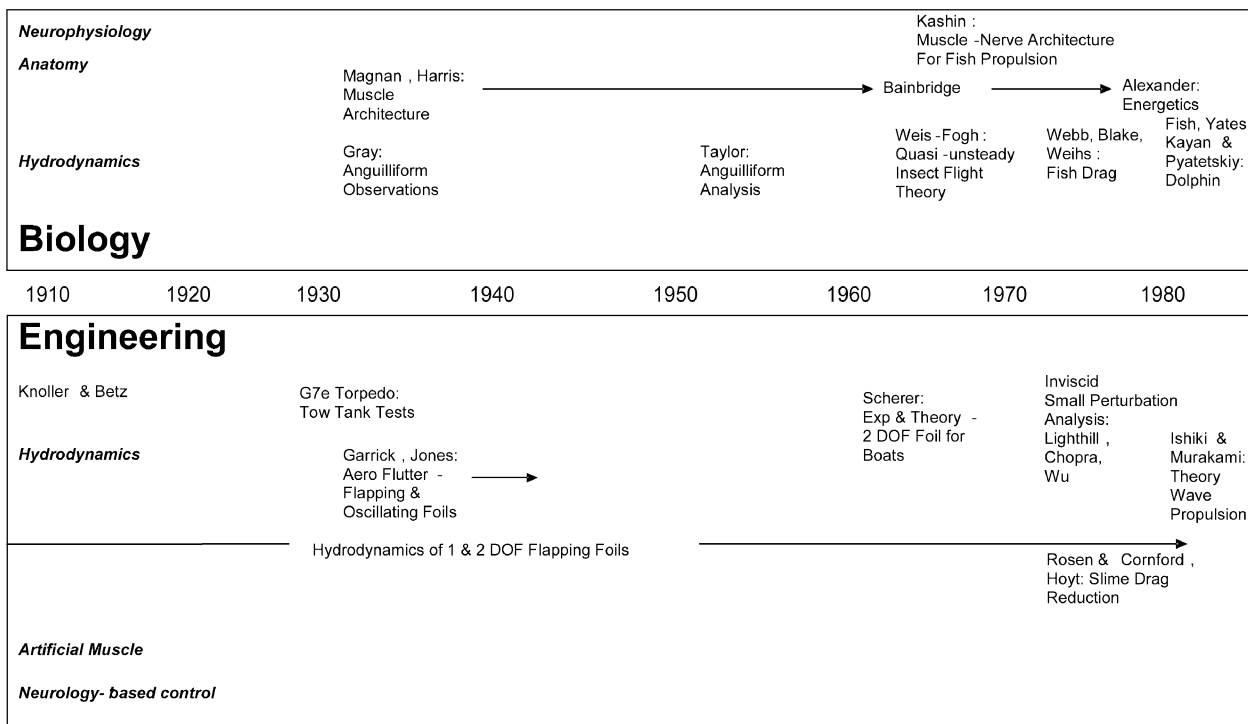
this paper. Note that the goal is not to build a robotic replica of animals. The goal is to distill the science from biology and implement that on existing platform components with a minimum of logistical and a maximum of operational impact.

#### D. Trends in Fish Locomotion Research

Animal systems tend to be very robust in a range of environments; they are adaptive, closed-loop systems with redundancy; and they are autonomous, economical, and optimized for their

environment. Based on the present objective of application of the distilled science from biology to AUVs, fish locomotion research can be divided into three periods culminating into an ONR Program, which attempts to integrate biology-based, high-lift hydrodynamics with AM and neurologically based control of pectoral fin devices, leading to a biorobotic AUV. These three periods are shown in Fig. 6(a)-(c). The first period [Fig. 6(a)], extending roughly up to 1990, is motivated by the assumption that swimming in nature employs mechanisms that are superior to

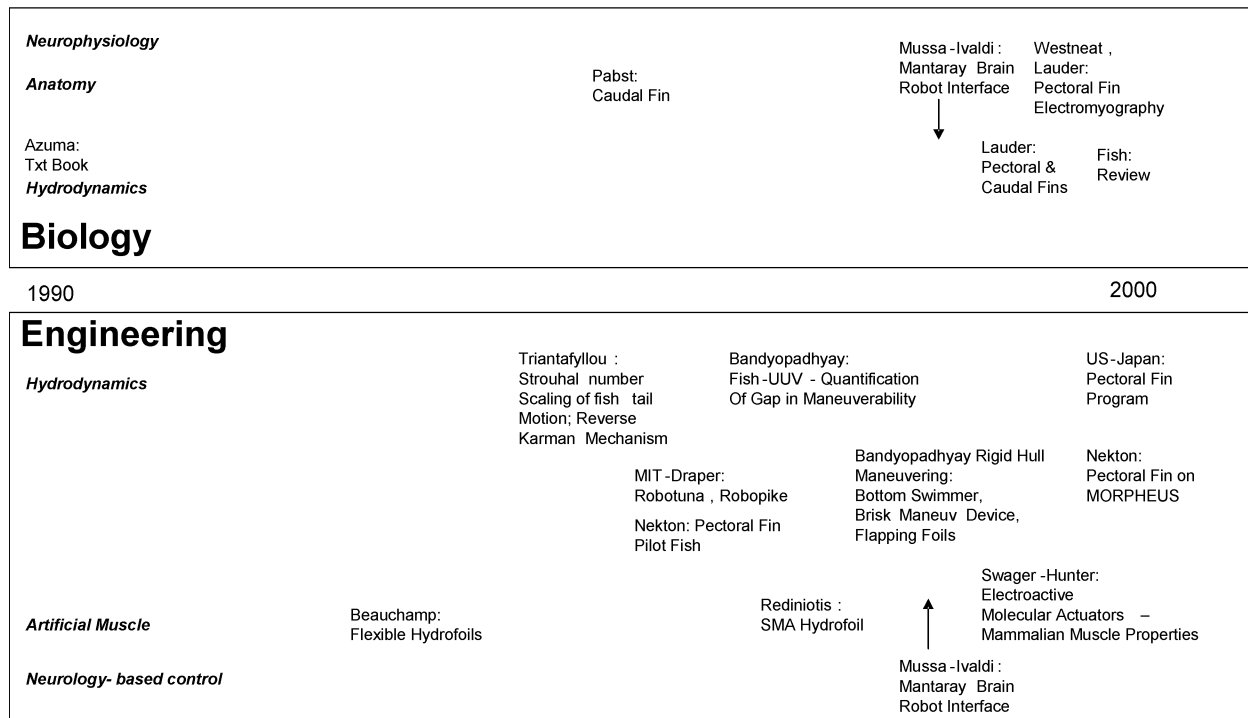
## Propulsion Dominant Early Period 1900- 1990: Inviscid Small Perurbation Analysis & Propulsion Large Amplitude Application of 1 & 2 DOF Flapping Foils on Flexible and Rigid Hulls



(a)

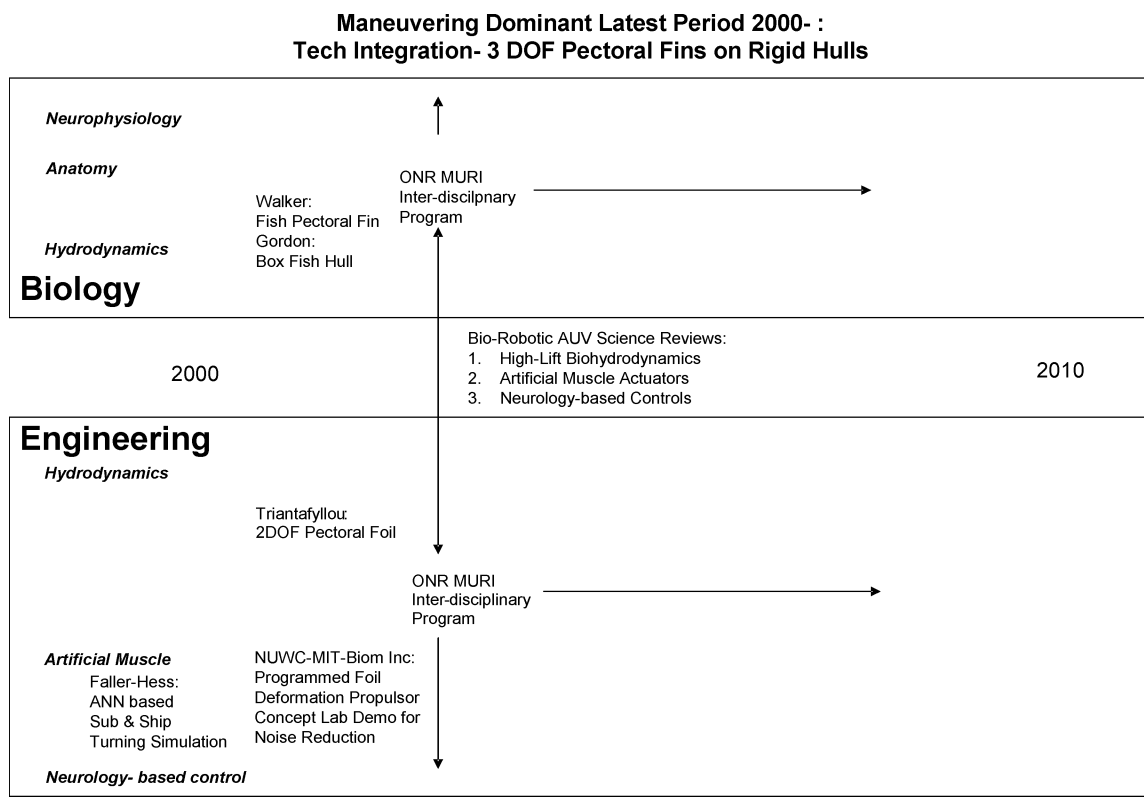
### Transitional Period of 1990s:

#### Propulsive to Maneuvering, Flexible to Rigid Hull, 1 DOF Flapping Foils to 2 DOF Pectoral Fins – Numerical Analysis, Vortex Dominated Flow Measurements & Platform Application



(b)

Fig. 6. (a) Propulsion and drag dominated early period of research: 1900–1990 [1], [54], [68], [70], [75], [77], [79], [94], [105], [106], and [131]. (b) Transitional period of research during 1990s with shifting emphasis from propulsion to maneuvering, flexible to rigid hulls and caudal to pectoral fin devices [2], [50], [51], [58], [70], [108], [112], [127], [131], [136], [139], [142], and [149].



(c)

Fig. 6. (Continued.) (c) Latest period of discipline integration for AUV maneuvering: 2000–2010 [38]–[53], and [153].

engineering. Mainly caudal fins have been examined for propulsion. Applications of such have been explored in torpedoes in Germany during WWII and in boats in the U.S. during the 1960s. Interest in biorobotics gained momentum during the 1990s, the second period [Fig. 6(b)]. This is the period of shift in emphasis to application, from propulsion to maneuvering, caudal to pectoral fin devices, and flexible to rigid hulls. The vortex-dominated unsteady hydrodynamics by now is firmly in place as the key characteristic of biolocomotion. Neurophysiologic aspects of fin motion also begin to show a link to the generation of unsteady hydrodynamic forces and moments. Independently, actuator material technologies, from shape memory alloys (SMA) to electro-active polymers, begin to emerge from chemistry laboratories to engineering products. The stage is thus set for the third, and current period of 2000–2010, as shown in Fig. 6(c). Here, the three sets of commissioned reviews [38]–[43], [44]–[49], [50]–[53], [151], written by teams of biologists and engineers, have distilled the sciences in the three component disciplines, namely bio-inspired, high-lift hydrodynamics [38]–[43] for application to AUV maneuvering, the fish pectoral fin neuroscience-based control engineering [44]–[49] of a pectoral fin device composed of AM, and AM technology for constructing pectoral fin devices [50]–[53], [151], respectively. This last period also marks the integration of the three disciplines to develop a pectoral fin for an AUV via the Multidisciplinary University Research Initiative (MURI) Program.

#### E. How to Measure Maneuverability

A mechanistic understanding of swimming follows. All underwater, land, or aerial platforms have two gaits of motion:

maneuvering and cruising. These motions have conflicting requirements and their balance is unique to each platform. The end of the Cold War signaled some shift in emphasis from a blue water to a littoral Navy. This can be interpreted to mean a need for a shift in the “balance,” namely to less of cruise (high-speed) and to more of (low-speed) maneuverability. (Later, this balance would be defined as a combined cruise-maneuvering index,  $\beta$  typical of any platform.) What is the characteristic of this balance in nature and engineering? This question has been considered in the context of fish [54]. Fig. 4 shows schematically the control fins of a fish that generate circulation varying over time and the length scales that define them. Such morphology of 30 species of fish has been considered. They are categorized as those known to excel in speed, in maneuverability, or an overlapping combination of speed and maneuverability. The first tends to be of open water pelagic variety, while the last is dominant in coral reefs. The scales of their control fins display systematic trends. A biorobotic application of dorsal fins on a rigid cylinder [54], [55] indicates the following. While manmade platforms tend to have moment-based maneuvering, which acts gradually over a long moment-arm, aquatic animals have force-based maneuvering mechanism acting near their center of gravity, which leads to a brisk response [1], [2], [56], [57]. On one hand, the control surfaces on manmade platforms experience steady flows around them and separation is generally avoided. On the other hand, the control fins on fish rely on unsteady vortex flows that generate large instantaneous levels of forces [1] via enhanced separation. Because of such needs, the fins of aquatic animals are characterized by an anisotropic muscle layout that has a neural controller [44]–[49].

Note that even rudimentary fish-based pectoral fins give an AUV excellent short radius turning and hovering ability at  $\sim 1$  kt

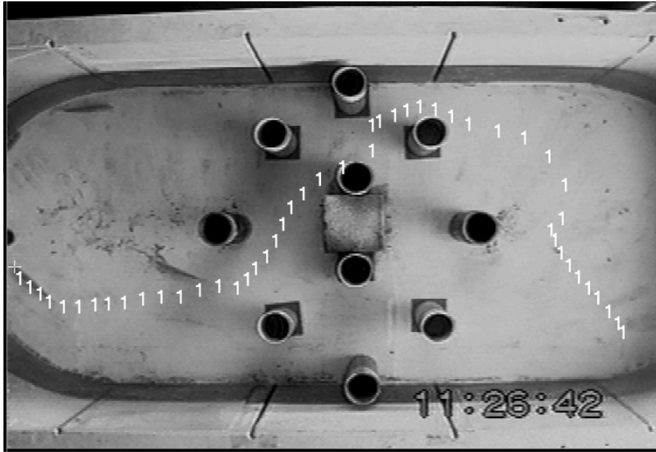


Fig. 7. Example of a digitized bluefish trajectory in a rectangular tank with pipes and maze cinder blocks [1], [54].

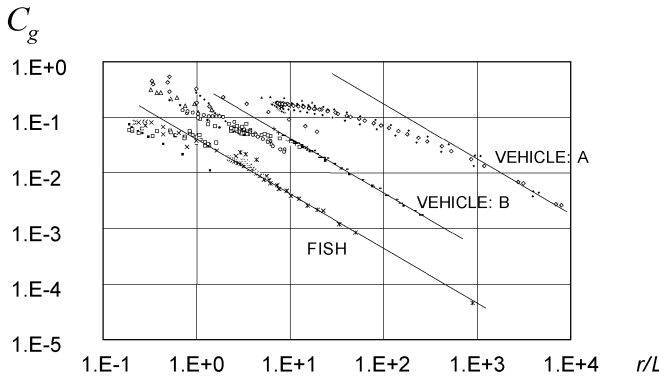


Fig. 8. Coefficient of normal acceleration of fish and manufactured vehicles [1], [54]. Solid lines: (1).

without any visible cavitation in shallow waters [58]. Conceptual analysis and early data [59] indicate that one of the high-lift mechanisms of tiny fruit flies ( $\sim 1$  mm), namely leading-edge dynamic stall, can be implemented on the propulsor of a tactical scale vehicle in a passive manner to lower rotational rate and noise while maintaining forward speed. The effects on cavitation and drag are unknown. Therefore, if the mechanism is judiciously applied, size and mass are not major issues.

To answer the question of what is the gap in maneuverability between fish and AUVs, experiments have been conducted with blue fish and mackerel in captivity [1] [54]. They are chosen because of their dexterity in both speed and maneuverability and because they are pelagic. Their trajectories in an obstacle-filled tank (Fig. 7) have been video-taped, digitized, analyzed, and compared with similar information (figure of eight trajectories) available from unmanned undersea vehicle (UUV) tests in the Atlantic Undersea Test and Evaluation Center (AUTEC).

The results of coefficient of normal acceleration  $C_g$  versus turning radius  $r/L$  are compared with two small underwater vehicles in Fig. 8. Here,  $C_g = (V^2/r)/g$  is the acceleration perpendicular to the path,  $V$  is total velocity,  $r$  is the radius of curvature in trajectory, and  $g$  is acceleration resulting from gravity.

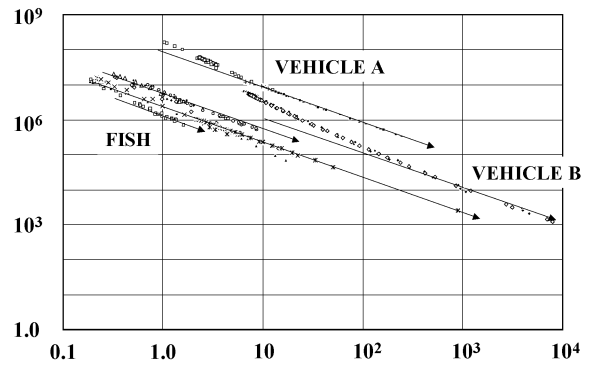


Fig. 9. Reduced coefficient of normal acceleration of fish and manufactured vehicles [1], [54]. Solid lines: (3).

Turning ability has improved over a few decades (earlier: Vehicle A; later: Vehicle B) and is attributable to improved control technology and not hydrodynamics. There is a large gap between the maneuvering capability of fish and the vehicles. There is a universal trend given by

$$C_g = \left( \frac{r}{L} \right)^{-1}. \quad (1)$$

However, (1) is followed in large turn radii only. Compared with underwater vehicles, fish can make the same radius turn at a normal acceleration that is lower by a factor that can be as large as 10.

The scaling law in Fig. 8 can be improved so that the wide Reynolds number range between natural and manufactured bodies is covered. Assume that the coefficient of normal acceleration during a turn is a function of inertia and viscous and gravity forces. Define, Reynolds number  $Re = VL/v$ , and an Internal Froude number  $Fr = V/\sqrt{gL}$ , where  $V$  is speed,  $L$  is length,  $v$  is kinematic viscosity of the fluid, and  $g$  is acceleration resulting from gravity. These two ratios can be combined as

$$\frac{Fr^4}{Re} = \frac{V^3}{L^3} \frac{v}{g^2}. \quad (2)$$

This combined parameter can be used to rescale the coefficient of normal acceleration shown in Fig. 8. The result is shown in Fig. 9. The solid lines in Fig. 9 are

$$\frac{C_g}{\frac{v}{g^2} \frac{V^3}{L^3}} \sim \left( \frac{r}{L} \right)^{-1}. \quad (3)$$

The inverse power trend (3) is now followed over a greater range of turn radius in both fish and vehicle data.

The significance of internal Froude number is as follows. Rewrite Fr as

$$Fr = \frac{V}{\sqrt{gL}} = \left( \sqrt{\frac{L}{g}} \right) \frac{V}{L} = \frac{1}{2\pi} \left( \frac{T}{L} \right). \quad (4)$$

Stated another way, this internal Froude number is a ratio of the time period of natural oscillation  $T$  like a pendulum [(5)], and the time it takes for the body to travel a distance equal to its length. This is reminiscent of a Froude number that is relevant to the wave drag of surface piercing bodies like ships and masts. It is interesting that the jets produced by fish, dolphins, or whales for propulsion are similar to the flow visualization of “fluttering”

TABLE III

RELATIONSHIP BETWEEN LENGTH AND FREQUENCIES OF TAIL BEAT AND NATURAL OSCILLATION OF DOLPHINS [65] NOTE THAT BOTH TAIL BEAT AND NATURAL FREQUENCIES DROP WITH INCREASING LENGTHS OF DOLPHINS

| Source of data  | [66]                              | [64]                      | [67]                      | [68]                      | [64]                        |
|---|-----------------------------------|---------------------------|---------------------------|---------------------------|-----------------------------|
| Dolphin species   | <i>Lagenorhynchus obliquidens</i> | <i>Tursiops truncatus</i> | <i>Tursiops truncatus</i> | <i>Tursiops truncatus</i> | <i>Pseudorca crassidens</i> |
| Length (cm)   | 209                               | 182 - 283                 | 251- 270                  | 230-265                   | 365                         |
| Average length $L$ (cm)   | 209                               | 240                       | 260                       | 247                       | 365                         |
| Measurements (mean) of tail-beat frequency $f$ at 6 m/s, chosen to allow comparison of trend (Hz) | No data                           | 2.65                      | 2.6                       | 2.56                      | 2.05                        |
| Calculated natural frequency $n$ (Hz) due to Pendulum Model                                       | 0.34                              | 0.32                      | 0.31                      | 0.32                      | 0.26                        |

of long and light strips in a liquid [60]–[62]. (Lightness can be considered equivalent to near neutral buoyancy for submerged bodies.) Conversely, heavy and short strips “tumble.” Note that [60] defines an (internal) Froude number, which is the reciprocal of the one given before. In [60],  $Fr$  defined in the present work has a high value for long and light strips, which flutter. Thus, fish, dolphins, and whales have high Froude number, but short heavy animals like beetles [63] have a low value of  $Fr$ . This allows reinterpretation of the conclusion in [63]. Because the flexibility of a humpback whale gives it a higher maneuverability than that of a whirligig beetle, which is rigid, the conclusion can be made that the internal Froude number is related to maneuverability.

The commonality of the wake pattern and the terms in the Froude number for fluttering objects suggests that a dolphin can be modeled as a simple pendulum. The dolphin swimming data [64] has been examined [1] [65]. Table III is a summary of the data sets based on lengths. It is proposed that the jet responsible for dolphin propulsion is analogous to the jet due to the predominantly side-to-side motion of fluttering long or light strips when dropped freely in air or water. The natural frequencies of dolphins calculated based on the following pendulum model are shown in Table III:

$$n = \frac{1}{T} = \frac{1}{(2\pi\sqrt{\frac{L}{g}})}. \quad (5)$$

For dolphins, the trend between the tail beat frequency  $f$  and speed  $U$  has a universal slope [64], [65]. Table III includes the tail beat frequencies ( $f$ ) at a swim speed ( $U$ ) of 6 m/s, selected to allow comparison between the data sets. Therefore, the relative values of frequencies is an indication of what the extrapolated value of  $f$  is at  $U = 0$ ; that is, the natural frequency. The table shows that the pendulum model reproduces the trend in tail beat frequency correctly: longer (older) dolphins of a species have lower tail beat frequencies than smaller (younger) dolphins at the same speed. The pendulum model is a fluid-structure coupling model. Its applicability to dolphins is an evidence of the presence of the mechanism of added mass resonance effect for enhancing propulsive efficiency. The body acts like a spring that stores energy and releases that in the shed vortices at appropriate phase. When the entire dolphin-swimming data based on their length are extrapolated to zero swimming speed, they agree with the calculated values of natural frequency closely. This

length consideration accounts for the seeming scatter in the data. In summary, buoyancy or lightness, length (slenderness), and Froude number appear to play important roles in maneuvering.

This information indicates that although cruise is dominated by inertial and viscous forces, and Reynolds number is a measure, turning maneuverability is dominated by inertial forces, and Froude number is a measure. As the definitions illustrate, Reynolds and Froude numbers incorporate the effects of length and velocity differently. Their “scaling up” is executed in engineering via empirical relationships. Computational fluid dynamics has been of limited help because of our inability to model turbulence at high Reynolds numbers [69]. Equation (2) combines these two conflicting effects and may be proposed as a Combined Cruise-Maneuverability Index

$$\beta = \frac{Fr^4}{Re} = \frac{V^3}{L^3} \frac{v}{g}. \quad (6)$$

The cruise-maneuverability index of any two underwater platforms may be compared based on the values of their  $V$  and  $L$ , since  $v$  and  $g$  remain the same for both. Now there is a physical basis to compare underwater platforms from nature and engineering in a  $V$  versus  $L$  coordinate, as shown in Fig. 10(a). Biologists have examined  $V$  versus  $L$  data of mostly swimming animals in the past, although no physical rationale has been offered as to why some systematic trend is observed or what that means [70]. Fig. 10(a) first shows the trend  $Fr = 1$ , which has a special significance to be explained soon, and also  $Fr = 0.1$  and 10, to indicate departures from  $Fr = 1$ . It also shows trends  $Re = 1, 10, 10^2, 10^3, \dots, 10^9$ . As proposed here, the  $Fr$  and  $Re$  lines indicate maneuvering and cruise abilities of a platform, respectively. Having laid out this basic framework, all aquatic natural and manufactured platforms are now compared, from the tiniest human spermatozoa ( $O(10 \mu\text{m})$  to low-speed AUVs, Russian diesel, and nuclear submarines ( $O(100 \text{ m})$ ). They fall in two clear categories. All manufactured platforms and most natural species, fall in the range  $Fr \leq 1.0'$ . Only a handful of species, namely marlin, barracuda, and bonitoes decisively fall in the range  $Fr > 1.0$ . Observe that they are in the “burst-speed” category, and not in normal cruise [70]. Fig. 10(a) also shows two fairly close burst-speed lines. The one on the left is the popular simplified  $10\times$  empirical line: burst speed  $V = 10L$ . The lower and steeper trend is the refined version because of Azuma ( $V = 7.8L^{0.88}$ : [70, eq. 6.3-20]). Comments on the quality of the burst-speed data and trend line follow. A recent reexamination

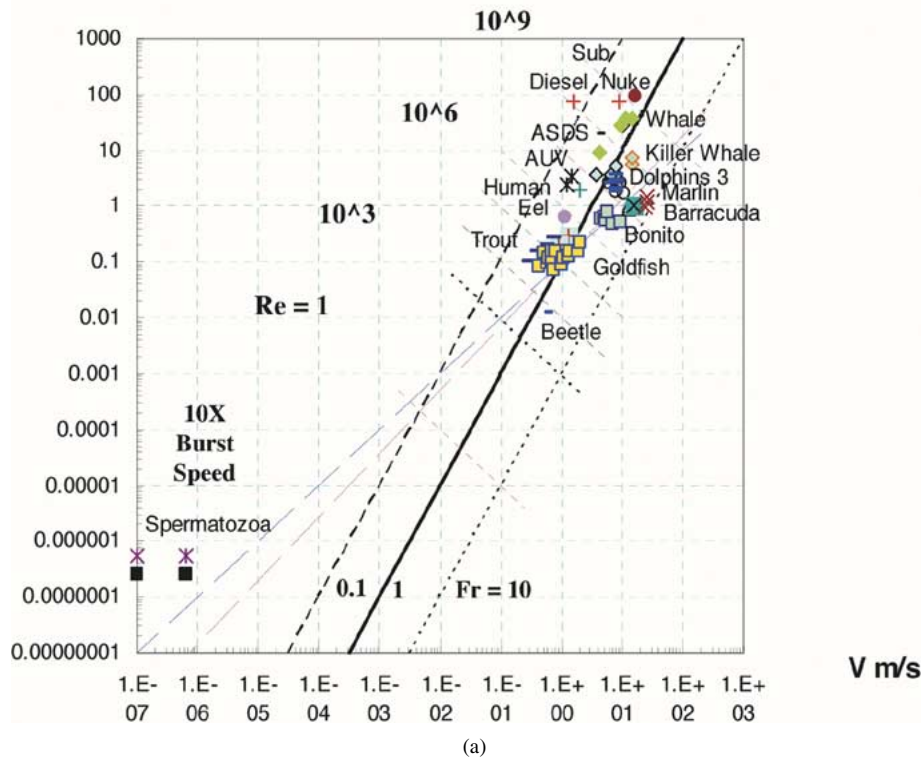
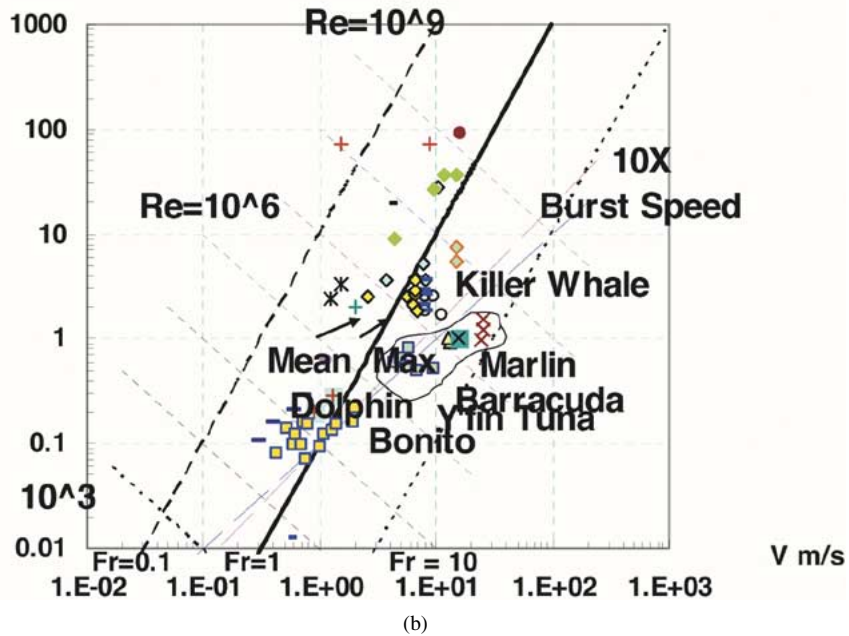
**L m****m**

Fig. 10. (a) Comparison of combined cruise ( $Re$ ) and maneuvering ( $Fr$ ) ability of sub-surface aquatic platforms in nature and engineering. The constant  $Re$  lines run diagonally left to right; the constant  $Fr$  lines run slightly slanted to the vertical. (b) Close-up of Reynolds number-Froude number relationship of aquatic platforms. Burst-speed trend lines are not well supported by data. Out of the two ( $10X$ ) burst-speed lines, the steeper line is a refinement. Refined measurements are needed to verify if maximum speed of the species, within the region marked by the peanut shaped perimeter, is truly as high as reported in literature and reproduced here. Recent measurements on dolphins have led to a downward correction in maximum and average speeds bringing them closer to the  $Fr = 1$  line [71].

of dolphins [71] indicates that they were overestimated in the past, thereby bringing the data sets closer to the  $Fr = 1$  trend.

Therefore, the question arises: Does the line  $Fr = 1.0$  indicate a physically significant barrier in underwater locomotion? The

line  $Fr = 1.0$  holds when the time period of natural oscillation equals the time taken by the platform to traverse its own length. Recall that in a surface ship design, crossing this line involves overcoming an abrupt increase in wave drag, and is considered

a barrier [72]. From the point of view of natural frequency, it is suggested that at speeds higher than that given by  $\text{Fr} = 1.0$ , a platform can be unstable. In the fully turbulent regime (high Reynolds number), conceivably, certain tendencies for instability can be overcome for transient burst speeds by implementing separation delay mechanisms. A persistent departure from natural frequency, as in burst swimming, is probably costly.

For fish swimming, the regimes of cruise can be denoted by  $\text{Re} = VL/v$ . The regime of  $\text{Re} < 1.0$  is dominated by viscous forces, and inertia force, in comparison, is negligible. The regime above may be discerned based on the nature of vortex shedding and in practical terms by the variation of tail strokes with  $\text{Re}$ . The measurements of tail beat frequency in mackerel [73], bluefish, bonito, mullet [74], goldfish, trout, dace [75], [76], sockeye salmon [77], and trout [78] have been analyzed, [70], [79]. A reduced frequency  $\sigma = 2\pi/(V/Lf)$  approaches a value of 10 independent of  $\text{Re}$  for  $\text{Re} > 10^5$ . The data indicates that, approximately, the flow is laminar up to  $\text{Re} \sim 10^3$ , transitional in the range  $10^3 < \text{Re} < 10^5$ , and turbulent for  $\text{Re} > 10^5$ , whence inertia force dominates viscous force.

Is the hydrodynamic mechanism of burst speed different from that for cruise speed? Alternatively, is it the same and is burst speed merely a consequence of higher muscle power mechanics? This work shows that burst speed is prevalent when  $\text{Fr} > 1$ ,  $\text{Re} > 10^5$ . This suggests that the species may be using some feature of turbulent flow. Normally, this would mean that boundary layer separation delay is a potential mechanism for producing higher thrust while lowering drag. Earlier, based on anecdotal observations of their speed, swimming animals like dolphins [80] have been studied for drag reduction mechanisms. However, the claim of their high-speed ability has been refuted recently [71]. The present Fr-Re representation, on the other hand, suggests that the species with extraordinary burst speed need to be studied for their potential use of separation control for thrust enhancement for transient durations.

The following remarks can be made from Fig. 10(b), which is a close up of Fig. 10(a). The recent data on the maximum and mean speeds of captive and free-ranging dolphins [71] are closer to the  $\text{Fr} = 1$  trend line and do not agree with the burst-speed trend lines based on fish. Whale data do not agree with them either. The burst speed of dolphins is only 20% higher than mean speed. Even marlin, barracuda, and yellow fin tuna data do not properly follow the burst-speed trend line, and even more so with the refined line. The premise of burst-speed muscles [81], or the premise hypothesizing the play of unknown drag reduction mechanisms [80] can be questioned. Similar to efforts [71] at the measurement of burst-speed of captive and free-ranging animals with higher precision, there is a need for conducting similar studies on accurate measurements of speeds of marlin, barracuda, and bonito.

To summarize, what the present mechanistic Re-Fr approach has done in Fig. 10 is identify quantitatively, based on a physical rationale, a wedge, namely for  $\text{Fr} > 1.0$  and  $\text{Re} > 10^5$ , where the species are known for high-burst speeds. These species are worth a closer look for mechanisms of separation control that could aid maneuvering and sprints to high-burst speeds.

In the absence of forward speed, minimum-turning radius is a useful measure of maneuvering. The ability of boxfish to make a small radius turn as compared with its length is depicted in Fig. 11. A comparison of this turning ability with that of other fish is shown in Table IV(a). The coral reef fishes, which have an

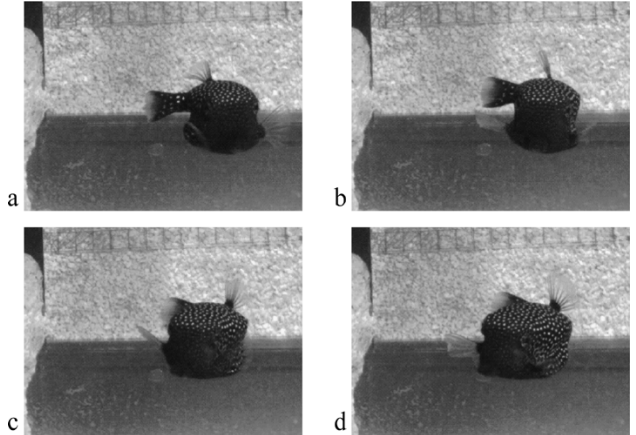


Fig. 11. Short radius turning ability of a boxfish in time sequence from a-d [82].

TABLE IV  
 (a) TURNING CHARACTERISTICS OF BOXFISHES [82]. (b) MEAN MINIMUM SIZE-STANDARDIZED TURNING RADIUS ( $r/L$ ) AND MEAN MAXIMUM AVERAGE TURNING SPEED (W) FOR BOXFISH UNDER DIFFERENT EXPERIMENTAL TREATMENTS [82]

| <i>Species</i>                     | <i>Common name</i>     | <i>L (cm)</i> | <i>Minimum turning radius r/L</i> | <i>Angular velocity w/L (deg/s)</i> |
|------------------------------------|------------------------|---------------|-----------------------------------|-------------------------------------|
| <i>Ostracion meleagris</i> [82]    | Blue spotted boxfish   | 11.6          | 0.001                             | 12.7                                |
| <i>Ostracion cubicus</i> [82]      | Yellow spotted boxfish | 4.7           | 0.001                             | 103.6                               |
| <i>Chaaetodon capistratus</i> [84] | Four eye butterflyfish | 4.3           | 0.08                              | 160.4                               |
| <i>Acanthurus bahianus</i> [84]    | Ocean surgeonfish      | 4.6           | 0.09                              | 114.6                               |
| <i>Thalassoma bifasciatum</i> [84] | Bluehead wrasse        | 5.7           | 0.08                              | 131.8                               |
| <i>Stegastes leucostictus</i> [84] | Beaugregory damselfish | 4.5           | 0.06                              | 206.3                               |
| <i>Carassius auratus</i> [85]      | Goldfish               | 6.6           | 0.26                              | 27.4                                |
| <i>Metynnis hypsauchen</i> [85]    | Silver dollar          | 6.1           | 0.66                              | 23.0                                |
| <i>Pterophyllum scalare</i> [85]   | Angelfish              | 5.9           | 0.41                              | 25.1                                |
| <i>Dineutus horni</i> [86]         | Whirligig beetle       | 1.25          | 0.24                              | 3542.4                              |

(a)

| <i>Treatment of fins</i> | <i>Population</i> | <i>r/L</i> | <i>w deg/s</i> |
|--------------------------|-------------------|------------|----------------|
| Control                  | 15                | 0.000552   | 183            |
| Median fin ablated       | 7                 | 0.000617   | 312            |
| Tail fin stiffened       | 5                 | 0.000089   | 101            |
| Both                     | 6                 | 0.000023   | 100            |

(b)

evolved advanced fin system, can turn at radii less than 10% of body length. The question may be raised if pectoral fins can play the prime role in turning [82]. Table IV(b) shows that it does.

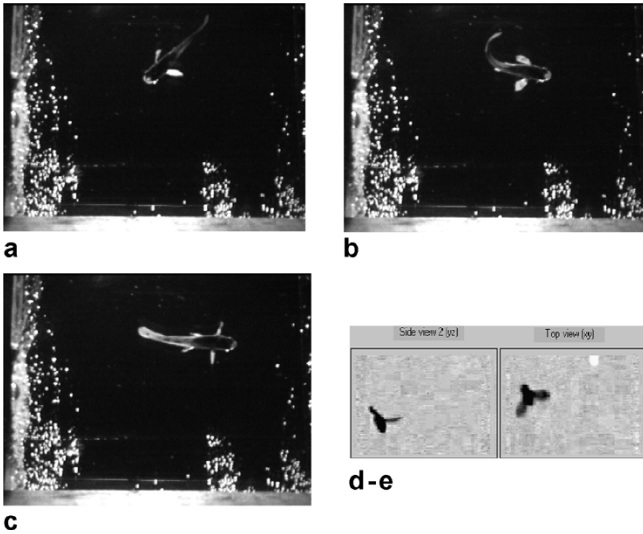


Fig. 12. (a)–(e) Examples of “terminal maneuvering” in guppy fish [82] (a–c) and fruit fly [89] (d–e). Top views shown. Time increases from a to c and d to e. The guppy fish is 2 cm long and makes a 90° turn in 70 ms and a 180 deg turn in 160 ms, which are equivalent to 4 turns/s in water. The fruit fly in d–e makes a 90° turn in 50 ms in 10 wing beats, which is a rate of 5 turns/s. The turns/s rate interestingly is similar in water and in air.

Although the present work focuses on the value of pectoral fins as a precision maneuvering high-lift device for cylindrical AUVs, the roles of the keel morphology of boxfishes in stabilizing the platform are woth examining [87]. Authors have mapped the vortex flow around models of four morphologically distinct boxfishes without the pectoral fins. Vortices of circulation similar to those in delta wings have been observed to form along ventrolateral keels in all of them. The vortices are positioned above the keel at positive angles of attack and, below, at negative angles. They propose that this is a mechanism for self-correcting pitching motions in the perturbed flow environment where these fishes live. The validity of this steady-flow investigation to an unsteady environment, and whether this mechanism holds in the presence of pectoral and other fins, remain to be established.

It has been pointed out that in Sturgeon, the pectoral fin and fish body interaction play a role in initiating a rising and sinking motion [88]. The pectoral fin is moved ventrally or dorsally to initiate a starting vortex, which induces a pitching moment thereby reorienting the body in the flow. The implication for AUVs is that, a pectoral fin, via its location near the nose, thereby giving it a greater control authority as compared with conventional foils near the tail, can initiate the low-speed maneuvering process faster via the production of the starting vortex and its interaction with the hull. This can be viewed as a mechanism for enhancing lift forces at low speeds by abruptly increasing the angle of pitch of the hull, which is normally a slow process to execute using the conventional foils at the tail. After this initiation by pectoral fins, the conventional control system for the tail foil can take over. This mechanism fills a need and is an alternative to the “brisk maneuvering device” of [55], although potentially less brisk [54]. Thus, it is emerging that a fish pectoral fin controlled by less than ten muscles could enable a rich repertoire of maneuvering at low speeds, namely initiation of rising and sinking, small radius turning, docking, undocking, and hovering. This justifies the need for

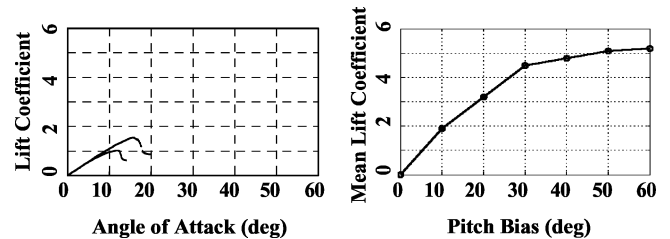


Fig. 13. Comparison of the coefficient of lift of a two-dimensional foil in steady forward motion (left: typical single foil and multicomponent slotted cambered foil results shown), and unsteady simultaneous motions of heave and pitch (right) [112]. Unsteady foil motion characteristics are: Strouhal number of oscillation = 0.60; maximum pitching angle = 25°; phase between heaving and pitching motion = 90°; pitch bias is the mean angle of attack.

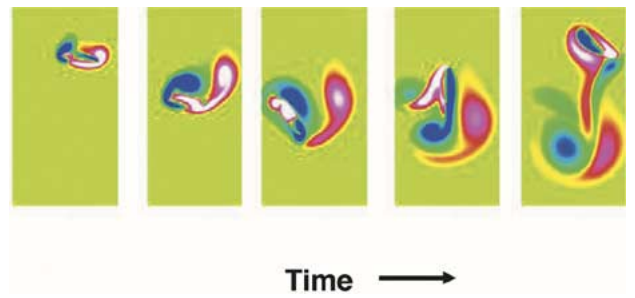


Fig. 14. Vorticity field snapshots around a two-dimensional heaving and pitching foil in quiescent environment simulating the flight of a dragon fly [91]–[93]. Observe the vortex-dominated unsteady flow due to leading and trailing edge separation and vortex formation. The vorticity formulation of Navier–Stokes equations is solved. Blue and red indicate vorticity of opposite signs.

neuroscience-based control architecture discussed later, which has a building block approach to complication.

#### F. Terminal Maneuvering

In a predator–prey dynamic, or when there is a looming obstacle, swimming and flying animals undertake a rapid change of course. Fig. 11(a)–(d) and Fig. 12(a)–(e) show three examples. Fig. 11(a)–(d) shows the limiting situation where the radius of turning is approaching a zero value. Fig. 12(a)–(c) shows a rapid change in direction. We hypothesize that the fish is abruptly producing considerable vorticity with attendant added mass effect that acts in a manner similar to ancient Greeks using halteres (hand-held weights) to enhance their long jump [90] or perhaps making use of any transient elastic property of water. Finally, Fig. 12(d), (e) shows a saccade of a fruit fly in the process of avoiding a crash on to the bottom wall. Little is known now about the terminal maneuvering shown in Fig. 12(a)–(e), which is outside the scope of this paper. It is curious to observe in Fig. 12 that both a guppy fish in water and a fruit fly in air make an abrupt 90° turn in roughly the same time, within uncertainties of measurement.

### III. HIGH-LIFT HYDRODYNAMICS TECHNOLOGY: SCIENTIFIC FOUNDATION

#### A. High-Lift Hydrodynamics

The coefficient of lift ( $c_L$ ) of a two-dimensional foil undergoing simultaneous heave and pitch motion is compared with that resulting from steady-forward motion, in Fig. 13. In the

TABLE V

(a) STATUS OF RELATIONSHIP BETWEEN ASPECT RATIO OF HIGH-LIFT FINS/WINGS OF FISH TO MANEUVERING AND PROPULSION [96].  
(b) KINEMATIC AND HYDRODYNAMIC MEASUREMENTS [96] OF PECTORAL FIN TURNING IN SUNFISH [101] AND TROUT [102]

| Exemplar species and their characteristics |  | <i>High (<math>\geq 3</math>)/Medium (~2) Aspect Ratio (AR)</i>  |  | Low (~1) Aspect Ratio<br><i>Bass, boxfish</i>  |
|--|--|--|--|--|
|  |  | <i>Low force</i>   | <i>High force</i>  |  |
|  |  | <i>Sharks, sturgeon, trout</i>   | <i>Surfperch, sunfish, some wrasses</i>  |  |
| Kinematics and forces                      | during steady horizontal locomotion                      | Wing-like fin held in complex three-dimensional conformation; effectively no angle of attack;<br>No thrust or lift generated; no muscle activity used to support fin | Kinematics described in 3D [97]; Forces [98, 99] measured  | Dorso-ventral and antero-posterior excursions roughly equivalent                             |
|  | during vertical maneuvering (dorsal–ventral)             | Posterior edge of fin used as flap to generate positive and negative lift and moments around center of mass rotating fish; muscles activated                         | No data  | No data  |
|  | during horizontal maneuvering (left-right); 20–150 deg/s | No data; limited fin excursions and very low left-right forces   | Left and right pectoral fins move asymmetrically: one fin generates lateral force, one thrust only [100] | No data  |
| Notes:                                     |  | Pectoral fin base is oriented nearly parallel to body axis   | Pectoral fin base inclined at approx. 45+ deg to body axis   | Very few experiments done; none measure forces; no maneuvering data; no muscle activity data |

(a)

| Variable   | Sunfish<br>$AR = 2.8$<br>Good maneuvering | Trout<br>$AR = 2$<br>Poor maneuvering |
|--|---|---------------------------------------|
| Angular velocity of body rotation (deg s <sup>-1</sup> )   | 10.9±2.0                                  | 13.5±2.4                              |
| Wake jet angle (deg)                                       | 91.6±5.5                                  | 121.4±5.0                             |
| Wake momentum, lateral component (g cm s <sup>-1</sup> )   | 1151.7±245.0                              | 42.6±8.8                              |
| Force, lateral (left-right) (mN)                           | 20.9±6.5                                  | 2.7±0.9                               |
| Lateral (left-right) force/Fin area (mN cm <sup>-2</sup> ) | 2.9±0.9                                   | 0.8±0.3                               |

(b)

steady case, at an angle of attack of 5°,  $c_L = 0.5$ , while by 15°, the foil stalls. On the other hand, in the unsteady case, at a pitch bias of 5°,  $c_L = 1$ , twice of that in the steady case; while at a pitch bias of 15°, the foil has not stalled and  $c_L = 2.5$ . In the unsteady case, maximum value of the lift coefficient is about five times larger than that in the steady case. Fig. 14 is a simulation of this unsteady flow, which is dominated by vortex dynamics [91]–[93]. Based on laboratory-scaled model studies of insect flight, it is known that several sources of lift are present. Unlike that in steady flow; they are delayed stall allowing for high angles of attack, and rotational lift and wake capture resulting from foil motion [24], [25], [93], and [94]. This set of mechanisms soundly supplants the earlier work [95] where while unsteady hydrodynamics were used to explain high lift, separated flow was not yet as clearly understood as a distinct beneficial part of the unsteady mechanism. A discussion of several devices that employ this unsteady high-lift mechanism follows.

### B. High-Lift Fins for Maneuvering and Propulsion

In general, pectoral fins of fish, much like the wings of fruit flies, appear to incorporate a high-lift mechanism via simultaneous heave and pitch motions, unlike that of caudal fins. There is a wide variation in the aspect ratio (AR) of such pectoral fins or wings in aquatic animals. AR is defined as the square root of the ratio of the square of the leading edge span length to the planform area. Based on three-dimensional flow, high, medium, and low aerodynamic values are 10, 5, and 1, respectively. For fish, the respective values are 3–4, 2, and 1. The following engineering question arises: Are low-aspect ratio flexible pectoral fins more efficient for maneuvering, and are large-aspect ratio rigid wings more efficient for propulsion, possibly by the measure of per unit of energy consumption? Table V(a) shows what data sets are needed to find an answer.

Table V(b) shows that trout have much lower (~1/3rd) levels of pectoral fin force as compared with those of sunfish but

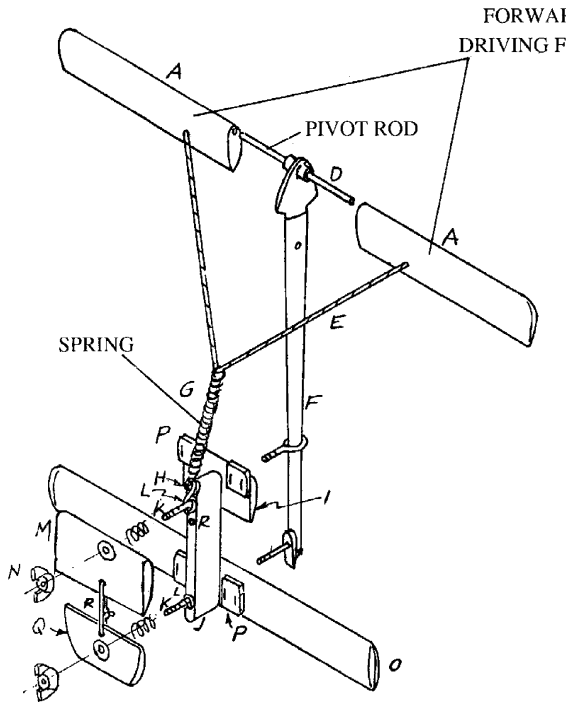


FIG. A Exploded View of AQUEON

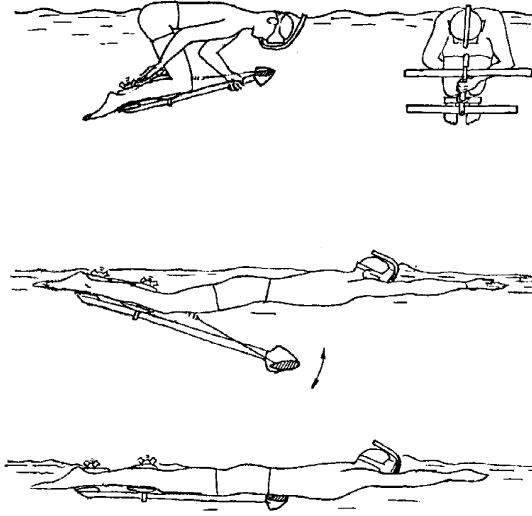


FIG. B Operation

Fig. 15. Gongwer's [103] human-powered AQUEON, implementing heaving and pitching motion of a foil to produce thrust. (a) Exploded view of AQUEON. (b) Operation.

compensates for the difference by using the flexible body to achieve the same angular velocity of body rotation. In other words, turning ability cannot entirely always be attributed to pectoral fins. Boxfish are less ambiguous in the sense that the body is rigid and turning is attributable to fins. Accurate documentation of the topology dynamics of pectoral fins is required to reveal why pectoral fins in Table V(b) having a similar AR do not produce the same levels of force/area.

### C. High-Lift Hydrodynamic Devices

#### Gongwer's Human-Powered AQUEON

Fig. 15 shows this device schematically [103]. For a short description, see Taggart [104]. It consists of two driving foils of aspect ratio 4.44, mounted on a pivot rod. A dolphin-type kick is used in the butterfly stroke of the swimmer to produce a heaving motion. The pivoting blade also undergoes a variable pitching motion. The amplitudes of heave and pitch angles and the difference in phase between the two determine the time-averaged thrust [105]. Propulsion performance using the characteristics of heaving and pitching foils [106] has been estimated [105]. Thrust and drag of the AQUEON are shown in Fig. 16. For an angle of attack of  $15^\circ$ , a heave of 75 mm, and a phase angle of  $45^\circ$  between heave and pitch, it is estimated that a speed of 5.7 kt can be reached for an expended power of 0.246 HP, and a propulsive efficiency of 50%.

### D. High-Lift Shallow Draft Boat

During the 1960s, there was an interest to build a shallow draft boat with flapping foil thrusters. The motivation was to avoid blockage in rotating propulsors or pump jet inlets of nozzles because of weeds. An analytical and experimental study of

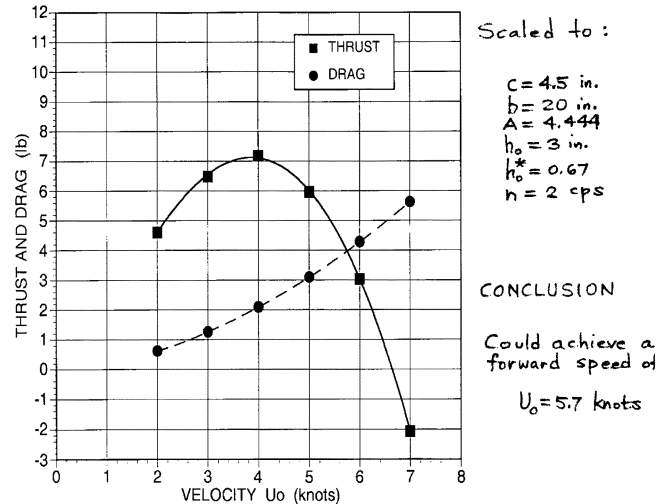


Fig. 16. Estimated [105] thrust and drag of Gongwer's [103] human powered AQUEON scaled to: chord = 11.25 cm; span = 50.8 cm; aspect ratio = 4.44; heave = 7.5 cm; heave/chord,  $h_0^*$  = 0.67; pitching frequency = 2 Hz; forward speed achievable = 5.7 kts.

heaving and pitching foils was conducted that led to the design of such a boat [106]. Payload was 2000 lbs. This foil device is shown in Fig. 17. Scherer concluded that, "an oscillating foil propulsor can provide efficient shallow water propulsion with a high degree of maneuverability." He added that, "the ultimate practicality of the system will depend more on the solution of the mechanical drive problems than with the hydrodynamic performance." A fish pectoral fin-based device made out of electroactive polymer is a solution to the mechanical drive problems of a linear foil as shown in Fig. 17, and maneuverability indeed is

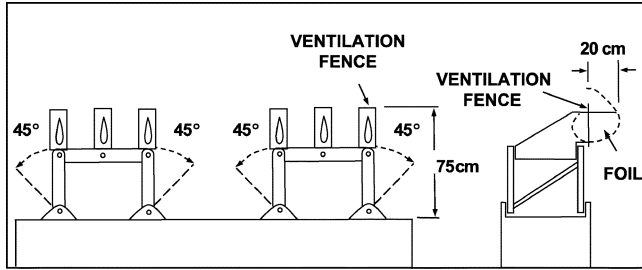


Fig. 17. Schematics of shallow draft boat using heaving and pitching foils. Maximum speed = 15 kts; efficiency = 0.64; coefficient of lift = 0.9 at stall [3], [105].

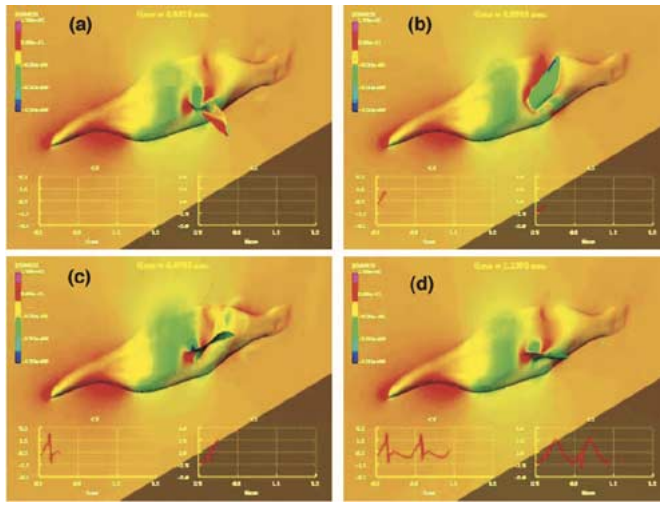


Fig. 18. Simulation [107] of pectoral fin based station keeping of a wrasse fish for times: (a) 0.501, (b) 0.576, (c) 0.678, and (d) 1.139 s. In each frame, lower left trace: coefficient of thrust; lower right trace: coefficient of lift; horizontal scales of time trace: 0.0–1.5 s; vertical scales of coefficients: −5.0 to 5.0.

the present motivation. The current biorobotic AUV effort can be seen as an evolution of Scherer's work.

#### E. Pectoral Fin Devices—Biological Studies and Engineering Devices

**1) Biological Studies:** A preliminary effort has been made to simulate the hydrodynamics of the pectoral fin of a wrasse fish [107]. The fin topology and the time-trace of the coefficient of lift force are shown in Fig. 18. The 3-D, time-dependent topology of fish pectoral fins that are, in fact, adaptive surfaces, has not yet been documented accurately. The pectoral fin topology is derived [108] from limited time traces of the motion of several marked points on the periphery of the fin, as shown later in Figs. 29 and 30. The simulation achieved station keeping at a stream speed of 0.45 m/s. However, the relevance of this simulation to fish station keeping should be treated with caution because in Sturgeon, during station keeping, both pectoral fin muscle electromyography and fin observations indicate a complete absence of muscle activity or fin movement [88]. This raises questions about the presence of a yet-unknown, station-keeping mechanism in fish not attributable to pectoral fins in general. In biofluid dynamics, speculations on mechanisms abound. Computational fluid dynamics has the potential to resolve the high-lift mechanism because several important

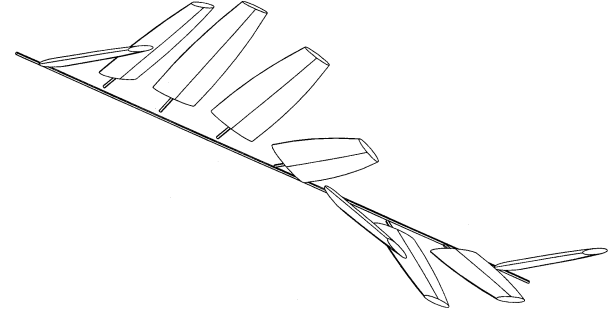


Fig. 19. Schematic of time sequence of a finite size heaving and pitching foil [3], [112] (also see Fig. 20).

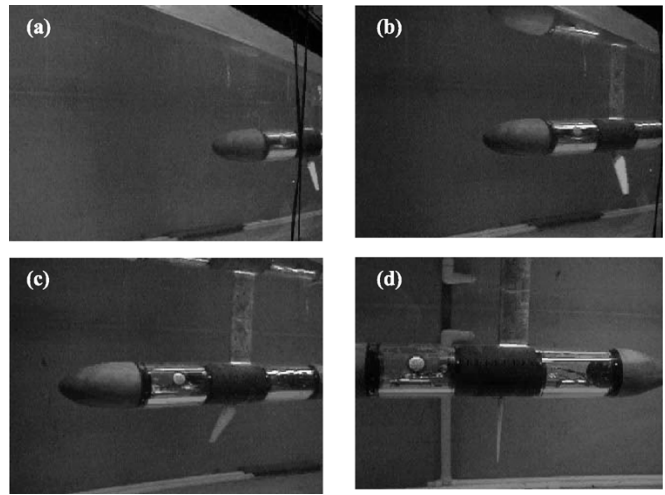


Fig. 20. Engineering development of a sealion wing-inspired heaving and pitching rigid foil. The time sequence (left to right) of a foil hanging from a cylinder in a tank, is shown [3], [112]. Observe the thrust producing dynamic configuration of the foil.

variables that cannot be measured can be simulated. There is a need to employ a code that inherently has the capability to compute accurately separated flows around moving 3-D and flexible surfaces and has been validated against reliable measurements, coupled with uncertainties that are both acceptable as well as accounted for. Large eddy simulation (LES) and detached eddy simulation (DES) techniques, as well as immersed body method (IBM), appear to have the capability to model the required separated fluid and moving structure interaction [109]–[111]. To date, scientists have not developed such computational codes for examination of biohydrodynamic mechanisms.

**2) Engineering Devices:** Considering the underdeveloped status of the hydrodynamic simulation codes, measurements on pectoral fin-based engineering devices assume importance. Figs. 19 and 20 show two-degree-of-freedom foil. In this experiment, the foils do not reproduce the animal fin topology accurately. Incorporation of twist would be an improvement. For flexible foils, an understanding of the elastic nature of animal fins is essential. However, simulation of biological features is not a goal. The objective is to distill the essential science mechanism and to implement only that on engineering products to create value as shown elsewhere [59]. Whether the final product looks, feels, or functions like any animal is immaterial.

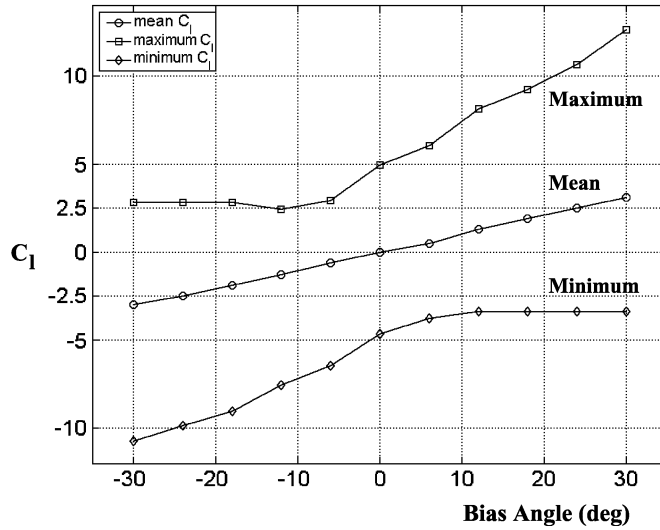


Fig. 21. Lift coefficients and bias angles of 3-D pitching and heaving foils [3], [112]. Maximum pitching angle range: 15 deg at mid-span; roll angle: 37° at midspan; at mid-span, Strouhal number St: 0.36. Observe the linear trend in mean lift coefficient, a high value of 2.6 at a bias angle of 30° and large instantaneous levels.

Fig. 21 shows results from Triantafyllou and coworkers [112]. The mean coefficient of lift continues to rise beyond a value of 2.6. A striking aspect is the production of large levels of positive and negative forces that could be useful to maneuvering.

#### F. Feasibility of Emerging Pectoral Fin High-Lift Hydrodynamics Technology

On January 2002, a pre-workshop was organized by ONR that gathered biologists, experimental and computational engineers, and academic and Navy propulsor designers to discuss if biology-based (primarily pectoral fin-based) high-lift hydrodynamics were suitable for underwater application [3]. See [153] for papers on the succeeding workshop. Hydrodynamicists and artificial muscle developers as well as researchers of neuroscience based control methodologies were commissioned to investigate a given test case. This activity involved the following. Consider a 0.53-m diameter and 5.3-m long AUV. Then, replace the existing propulsor by pectoral fin propulsors that do not rotate about the vehicle axis but heave and pitch about the individual foil axis. Determine the attainable vehicle speeds and compare the feasibility of various artificial muscle technologies. Table VI shows that speeds of 3.5–15 kts can be reached. The noise spectrum would be narrower (Fig. 45) and further improvement in speed might be possible via flexible fins and by adding more of them, as discussed in Section VIII.

#### IV. ARTIFICIAL MUSCLE ACTUATOR TECHNOLOGY

Actuators that convert electrical to mechanical energy are considered. Here, a comparison is made of the basic properties of animal muscles and artificial muscle actuators. The strategy for defining the required properties of artificial muscles, inspired by the ability of dolphins to detect buried mines is discussed. The salient features of the development of conducting electroactive polymers, starting from their so-called molecular design, follows. Finally, a comparative assessment of the suitability of

TABLE VI  
ESTIMATED [3], [112] SPECIFICATION OF PECTORAL-FIN INSPIRED AUVs  
BASED ON MIT OCEAN ENGINEERING TOW TANK TWO-DEGREE OF  
FREEDOM FOIL MEASUREMENTS: ONR TEST CASE RESULTS

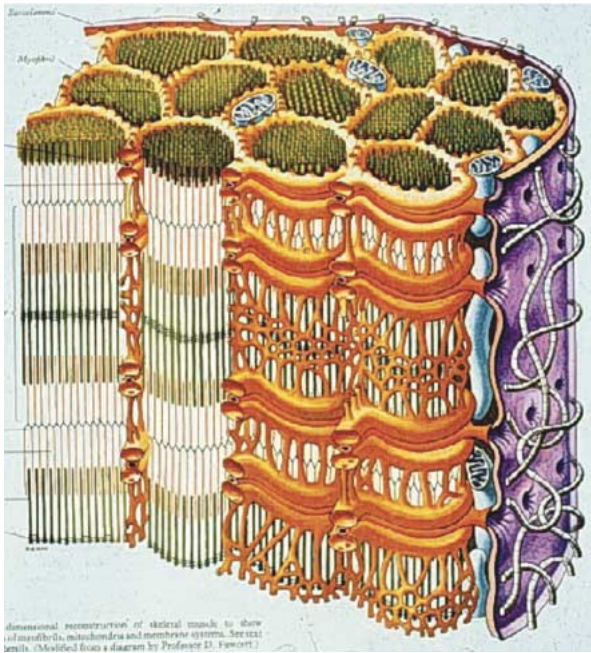
| Designation | UVU: 5.3 m long x 0.53 m diameter,<br>coefficient of skin friction = 0.003 | Foil description                                     | Foil excursion | Power  | Force      |
|-------------|--|--|----------------|--------|------------|
| Fast        | 7.5 m/s (15 kts)   | 4 foils 16.5 cm x 7.5 cm ( $Re = 5.6 \times 10^5$ )  | 15 cm at 12 Hz | 4.5 kW | 400 N/foil |
| Slow        | 1.8 m/s (3.5 kts)  | 4 foils 16.5 cm x 7.5 cm ( $Re = 1.35 \times 10^5$ ) | 15 cm at 3 Hz  | 62 W   | 20 N/foil  |

various muscles to the needs of the ONR UUV test cases [3] will be made.

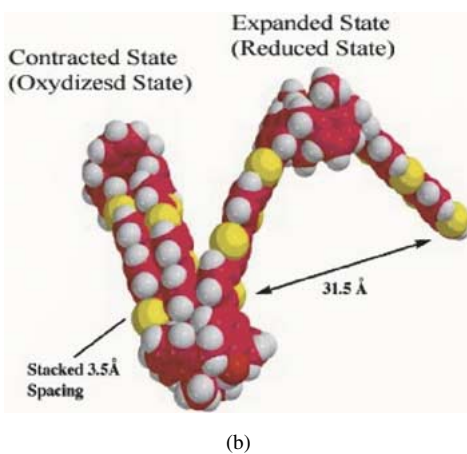
A natural muscle is a molecular motor that resembles a linear motor [113]. It can shorten actively but requires an external force to stretch. The characteristics of muscles have now been related to their subcellular structure [114]. Stated simply, muscles may be viewed as a series of 2.2  $\mu\text{m}$  long basic building blocks called sarcomeres. They have a parallel woven structure of segmented thin (actin) and thick (myosin) filaments laterally joined by cross-bridges. More numbers of cross-bridges tie the thick and thin filaments when load is higher. Chemical agents are produced to connect the cross-bridges [113]. As a series, the sarcomeres carry the same levels of force while the strain rate becomes cumulative. Advanced artificial muscle research is currently attempting to make polymer building blocks at a molecular level that resemble the structure of natural muscles [151]. This opens the possibility of designing artificial muscles that have a host of properties tuned to the needs of AUVs.

Electroactive polymers (EAP) can generally be of ionic or field types depending on whether a flow of ion or an external field controls the motion, respectively [115]. Operationally, the ionic types require <5 V, ~1 A and have an electromechanical efficiency of <1%. The field types on the other hand require 1 kV for a 20- $\mu\text{m}$ -thick muscle, <0.5 mA, and have an efficiency of 20%–30%. Because field type EAPs act like capacitors, an energy recovery circuit would increase their efficiency far more than is possible in the ionic type.

Animal muscles can be viewed as a closed-loop system of subsystems at the microscopic level (molecular or cellular). The following are examples of subsystems: power supply, including fuel, generation, storage and distribution; sensors; actuators; mechanical supporting structures; and information processing logic computers and communication networks. The ideal goal of making such self-sustained muscles is not our target. Fig. 22(a) is an example of the complexity of skeletal muscles. From an engineering point of view, the following features may be noted: it is composed of aligned fibers and fibrils; it has a modular construction; and it has encapsulation. It also has local



(a)



(b)

Fig. 22. (a) Schematic of mammalian skeletal muscle [3], [116]. (b) The structure of a single molecular actuator of bithiophene monomer compound. The left side shows the molecule in its contracted (oxidized) state and the right side at its expanded state (reduced). In macroscopic scale, as in biology, the artificial muscle also has arrays of billions of such individual actuators. Muscle fabrication generally involves these steps: synthesis of monomers, which involves building of the molecule, adding a hinge or rod via a series of chemical reactions (example: thiophene at the right position to hinge); electro-deposition to form a long chain polymer; followed by rolling of the solid film [117], [151].

energy storage capability and integrated displacement sensors and force transducers. Additional features include controllable subunits allowing force and displacement to be scaled and a fast response resulting from integrated construction. These observations are being used as guidelines for the development of artificial muscles [Fig. 22(b)]. Its fundamental similarity with biology can be expressed as, “Like natural muscles, the macroscopic actuators are assemblies of billions of individual nanoscale actuators” [118]. Compared with mammalian muscles, fish muscles have little sensory feedback and, therefore, their engineering replication might be feasible.

Swimming and flying animals are evidence of the feasibility of unsteady high-lift hydrodynamic mechanisms in the context

TABLE VII  
COMPARISON OF THE PROPERTIES OF MAMMALIAN AND ARTIFICIAL MUSCLES  
WITH CLASSICAL SOURCES OF POWER [3], [116]

| Mammalian skeletal muscle                     | Strain %                                       | Stress MPa                  | Reaction time | Cycle life        | Density            | Fracture toughness   | Power kW/kg |                    |
|---|--|-----------------------------|---------------|-------------------|--------------------|--|-------------|--------------------|
| SMA: Ni-Ti shape memory alloy                 | < 1%   | 10                          | 20            |                   |                    |  |             |                    |
| Electroactive Ceramics                        |  | 30-40 MPa                   | 235           | 0.35              |                    |  |             |                    |
| Internal Combustion                           |  |                             | ms            | ms                |                    |  |             |                    |
| Electric: High Rev                            |  |                             | s-min         |                   |                    |  |             |                    |
| Electric: Direct drive                        |  |                             |               | > 10 <sup>9</sup> |                    |  |             |                    |
| Artificial Muscle: Polypyrrole                |  |                             |               |                   |                    |  |             |                    |
| Artificial Muscle: $\pi$ -stacked (predicted) | > 20   | 7, 2 typical                |               |                   |                    |  |             |                    |
|   | > 2  | 34                          |               |                   |                    |  |             |                    |
|   | ms-s   | ms-s                        |               |                   |                    |  |             |                    |
|   | Not known                                      | > 10 <sup>5</sup>           |               |                   |                    |  |             |                    |
|   | I-2.5  | I-2.5                       |               |                   |                    |  |             |                    |
|   | Resilient, Elastic                             |                             | Fragile       | Elastic           | Resilient, Elastic |  |             |                    |
|   | 0.04; Fuel: I MJ/kg; energy source: electrical | 0.01                        | 0.5           | I                 | 50                 | 0.05; Fuel: 20-40 MJ/kg; Meat-Food Processing cost: \$5/kg |             |                    |
|   | > I (nano-structured); energy source: Chemical |                             |               |                   |                    |  |             |                    |
|   | > 30   | 3 / 20 with energy recovery |               |                   | 30                 |  | 3           | 30-35 Efficiency % |

of a realistic platform. Animal muscles show that a closed-loop assembly of the above-mentioned subsystems and the attainment of their high energetic and mechanical properties are feasible. The energetic and mechanical properties of animal muscles have served as a benchmark for artificial muscles (Table VII).

Table VII [3], [116] compares the state of the art of the properties of mammalian skeletal with a variety of artificial muscles. The projected properties of the  $\pi$ -stacked muscle match or exceed those of the mammalian skeletal muscle benchmark. However, an approach is to first determine the mechanical properties needed for constructing pectoral fins for AUV application, and then use molecular design principles to engineer artificial muscles that optimize those properties, whether their exact counterparts exist in nature or not. In fish, different types of muscles produce different functions. Similarly, artificial muscles might have to be tuned to the dynamics.

The following plan has been devised to determine the required mechanical properties. The various Defense Advanced Projects Agency Controlled Biological Systems (ONR/DARPA

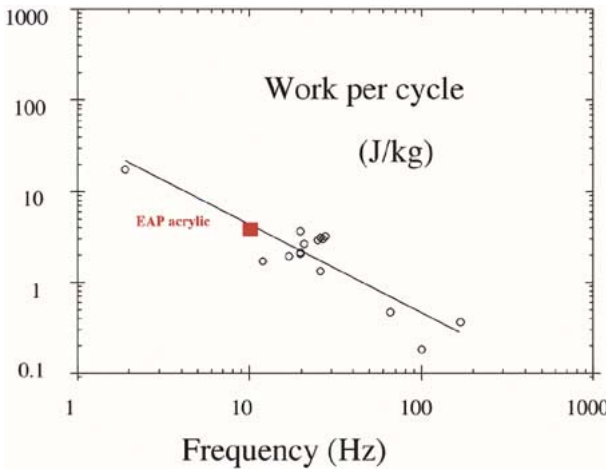


Fig. 23. Preliminary [120], [121] EAP results (filled square) compared with mass specific muscle work per cycle for vertebrate and invertebrate muscles (open circles).

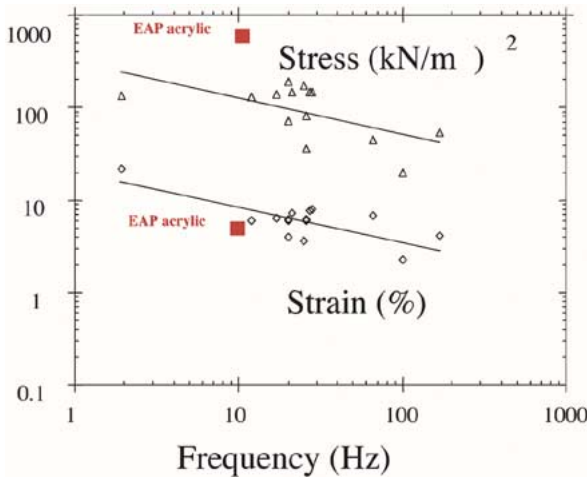


Fig. 24. Preliminary [120], [121] EAP data (filled square) compared with vertebrate and invertebrate muscle.

CBS) Biosonar Programs [6], [7], and [119] have made progress in understanding how dolphins detect buried underwater objects and in the development of engineering products. A multidegree of freedom of data on the motion of instrumented dolphins has been collected [119]. The following control study is in progress [152]. The successful AUV named REMUS is being simulated to determine if it could track the reference dolphin trajectory. The simulated REMUS would be “fitted” with simulated pectoral fins whose performance has now been documented in tow tanks. Such a biorobotic re-engineered REMUS would then be simulated to determine what characteristics of the pectoral fin would allow the reference trajectory to be matched. The accurate validated computational fluid dynamic and structural simulation of such pectoral fins would provide the benchmark mechanical properties that the desired artificial muscle would have to match. The simulation of such a biorobotic REMUS, when combined with the model of biosonar, would function like a rigid hull cylindrical and mechanical dolphin. This simulation should help the understanding of littoral mine clearance.

Figs. 23–25 compare the status of EAP artificial muscles with that of natural muscles [120], [121]. The EAPs fall within the ranges of natural muscles in mass-specific muscle work per

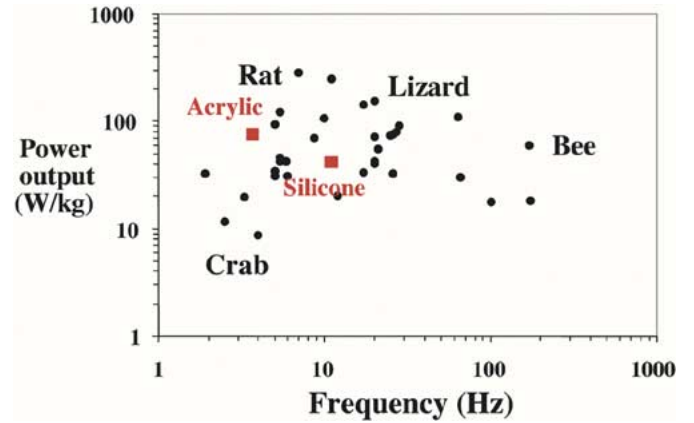


Fig. 25. Preliminary [120], [121] EAP data (filled squares) compared with mass-specific power output of natural muscles.

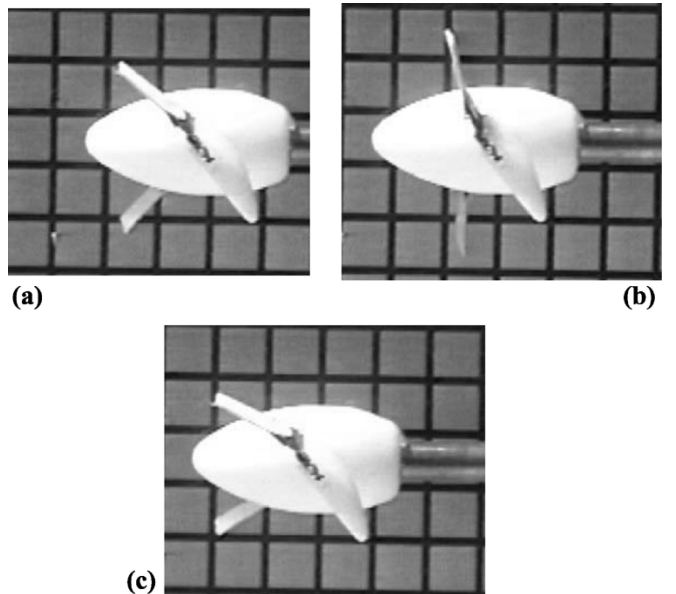


Fig. 26. Programmable propulsor blades made of artificial muscles [127]. Observe the variable cambering. Input pulse forms and nature of cambering are as follows. (a) Bipolar [Fig. 27(a)]: muscle is flat. (b) Positive unipolar [Fig. 27(b)]: muscle is cambered negatively; negative lift—reverse thrust. (c) Negative unipolar [Fig. 27(c)]: muscle is cambered positively; positive lift—forward thrust. Power supply to muscles: 100 Hz and 7 V. Such high frequency leads to cambering without oscillation and bubbles. Grid is 1-cm × 1-cm.

cycle and in power output; the stress levels are higher, but strain levels are lower. Both natural and artificial muscles should be evaluated using a workloop method that replicates the dynamic functional environment.

Conducting polymer actuators based [122], [123] on electrochemical dopant intercalation (molecule insertion) have been developed [50], [117], [124], [125]. Actuators have been developed that use “carbon single-walled nanotube sheets as electrolyte-filled electrodes of a supercapacitor” [118]. These nanotube sheet actuators are arrays of nanofiber actuators much like natural muscles [126]. The macroscopic actuators, like natural muscles, are assemblies of billions of individual nanoscale actuators. The contracted and expanded state of such an individual molecular actuator is shown in Fig. 22(b). The carbon nanotube actuators perform in saltwater and at low frequencies; they have the potential to convert mechanical energy of ocean waves into

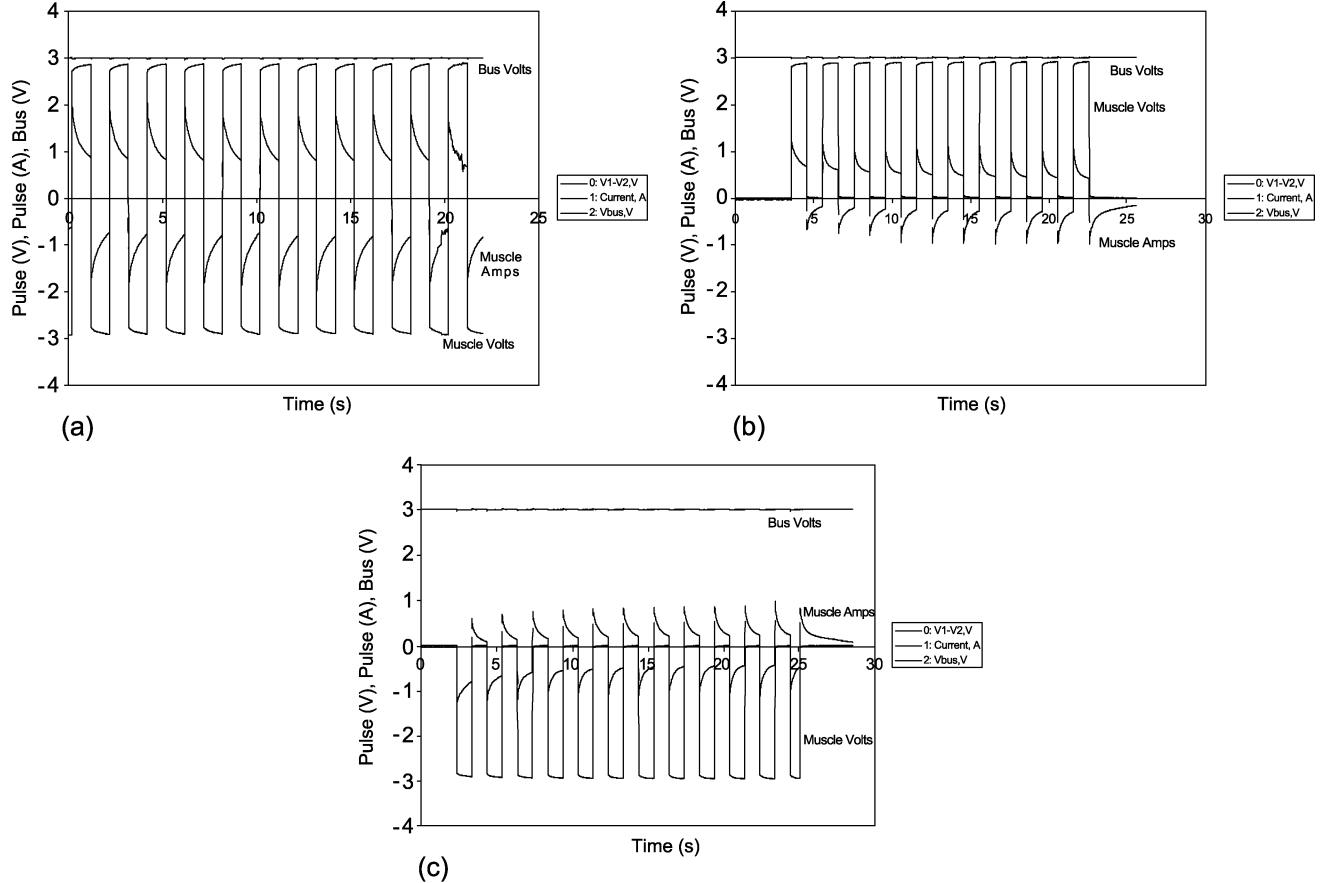


Fig. 27. Control pulse forms for cambering propulsor blades [127]: (a) bipolar, (b) positive unipolar, and (c) negative unipolar. Muscle: MS-417 with cloth backing; motion of muscle: (a) predominantly large amplitude oscillations from flat to large cambering; (b) predominantly flattens with minor oscillations; (c) predominantly cambered with minor oscillations (no bubbling, 3 V, 1 Hz, duty cycle 50%).

electrical energy. Carbon nanotube actuators have the potential to be useful as AUV pectoral fin muscles.

Because carbon nanotubes are made of carbon molecules, they are of nanometer scale. Another characteristic is their strength. They are tubular and not flat and good conductors of heat and electricity, since they are made of carbon molecules. Because of their superb conductivity, they have a potential in artificial muscle resulting from ease of charging and use as electrodes without added stiffness. When coiled and attached to a substrate, the composite would be strong and yet flexible. The longest tube made as of 2003 is 100 mm and the bulk cost is \$0.5 M/kg. Progress will accelerate when cost goes down.

Several issues need to be considered to determine the viability of electroactive polymer actuators. The cycle life needs to be  $> 10^6$  both when a dc load is present and when it is not. How much of the electrical input power is converted to mechanical power is measured by electromechanical efficiency. In monomers like polypyrrole and polyanieline, this is 1%–20%, which is good for small strain. In conducting polymer molecular actuators (CPMA) [50], [117], [124], this is 30%–70%, which is excellent. The CPMA operate in saltwater, but the longevity is not known. The interference of hydrolysis with polymer function can be reduced via encapsulation and controlled electrolytes in the muscle. Fabrication difficulties are believed to be minor. Polymer synthesis and manufacturing improvement are needed to increase bandwidth to 20–100 Hz. Higher density of electrical contacts, higher ion diffusion rates

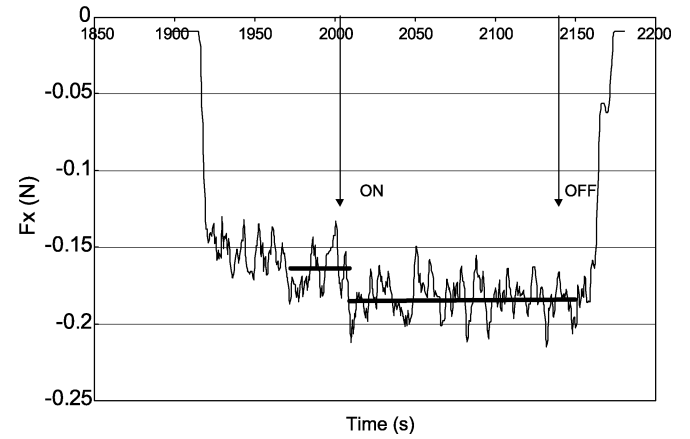


Fig. 28. Comparison of thrust signature during active cambering using a two-bladed propulsors [127]. Value of RPM is 520. Negative  $F_x$  indicates positive thrust. The muscle is MS-417 with cloth backing, power is 3 V, 1 Hz (bubbles are not produced during these measurements), and pulse form is negative unipolar, producing a positive cambering. Observe a 15% increase in thrust due to active cambering.

to propagate through polymer, perhaps through the use of carbon single-walled nanotube papers, and lower internal resistance to increase the rate of charging, are needed for further improvement of conducting polymer molecular actuators.

An alternative to the use of artificial muscles for building pectoral fin actuators would be to scale the “origami”-folded,

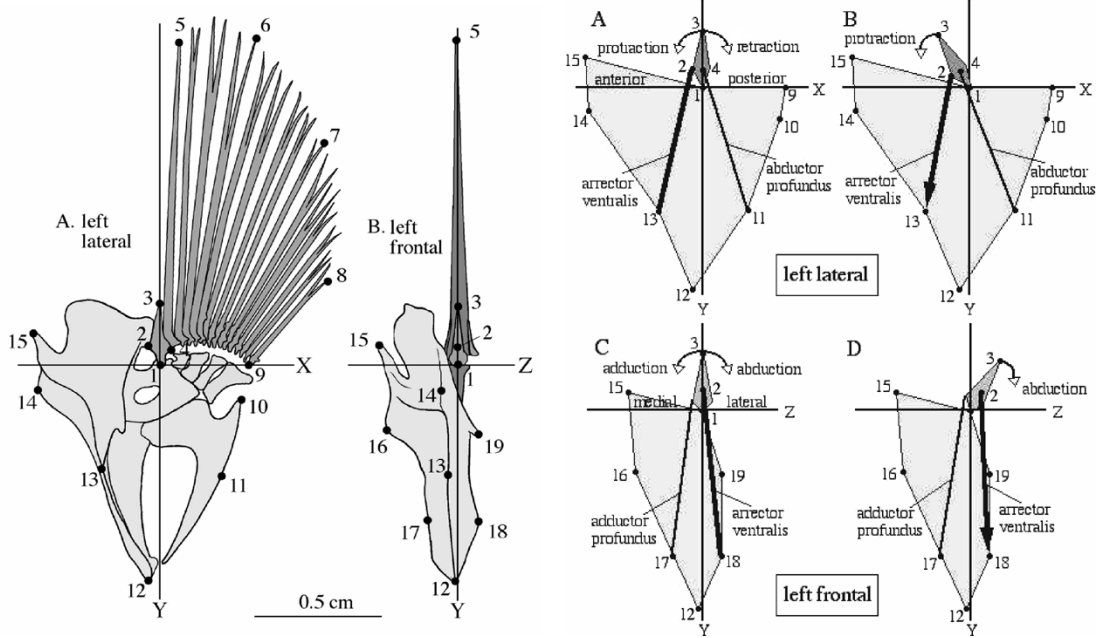


Fig. 29. Musco-skeletal morphology of pectoral fins of *Gomphosus varius* (left two) and its mechanical analog (right A–D) [134].

metal wing-fuselage “hinge” structure of MFI that has no rotary bearings and is used to produce the figure-of-eight wing motion [20]. This is a hingeless resonant joint, which seems to exist in nature [89]. Such a mechanism, not necessitating any motor, bearing, or seal, could be leak-proof and of value to underwater application.

#### A. Exploring the Value of Artificial Muscle-Like Actuators for Propulsors

An alternative biorobotic application of pectoral fins is sought. The value of AM technology in conventional underwater propulsors has been explored in NUWC [127], [128]. Section VIII shows that in conventional propulsors, noise arising from three sources can be reduced if rotation per minute (RPM) is reduced via high-lift foils, while keeping forward speed unchanged. There is a need to explore how the high-lift mechanisms of flying and swimming animals can be implemented on existing propulsors via the use of appropriately developed artificial muscles. Because such mechanisms are unsteady, they would require the availability of an active blade-cambering technology. Using recently developed ionic electroactive polymeric composite membrane muscles, the potential of such a digitally amenable technology has been demonstrated on a small laboratory propulsor. Fig. 26(a)–(c) shows the active cambering of blades in water resulting from the pulse forms shown in Fig. 27(a)–(c). These camberings are achieved digitally. Fig. 28 shows that active cambering can lead to an increase in thrust of 15%. A controllable lift (controllable pitch and camber) propulsor producing 15% additional thrust, compared with a similar conventional thrust at the same RPM, can be operated at a 7% lower RPM to produce the same thrust. This could lead to approximately a 1-dB reduction in directly radiated blade tonal noise resulting from decreased flow velocity over the blade sections. The primary value of active cambering may be in the improvement of propulsor and noise performance in off-design (off-cruise) conditions such as maneuvering.

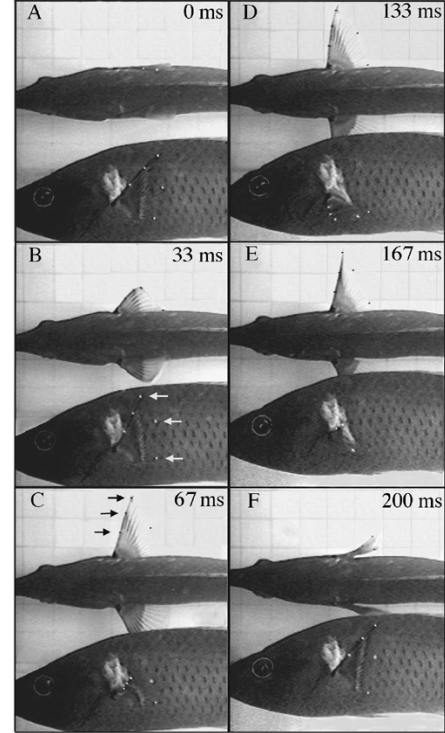


Fig. 30. Video images [134] of pectoral fin locomotion of *Gomphosus varius*. Note the three-dimensional time-dependent topology actuated by a set of six muscles, whose electromyogram synchrony is shown in Fig. 31.

#### V. NEUROSCIENCE-BASED CONTROL: EMERGING SCIENCE AND TECHNOLOGY

Considering control laws, attaching pectoral fins to a rigid cylinder creates an unconventional engineering problem because of the complexities of forces and moments of the fins and the nonlinear dynamics of the vehicle whose Reynolds number might also be changing. Pectoral fin forces and moments are

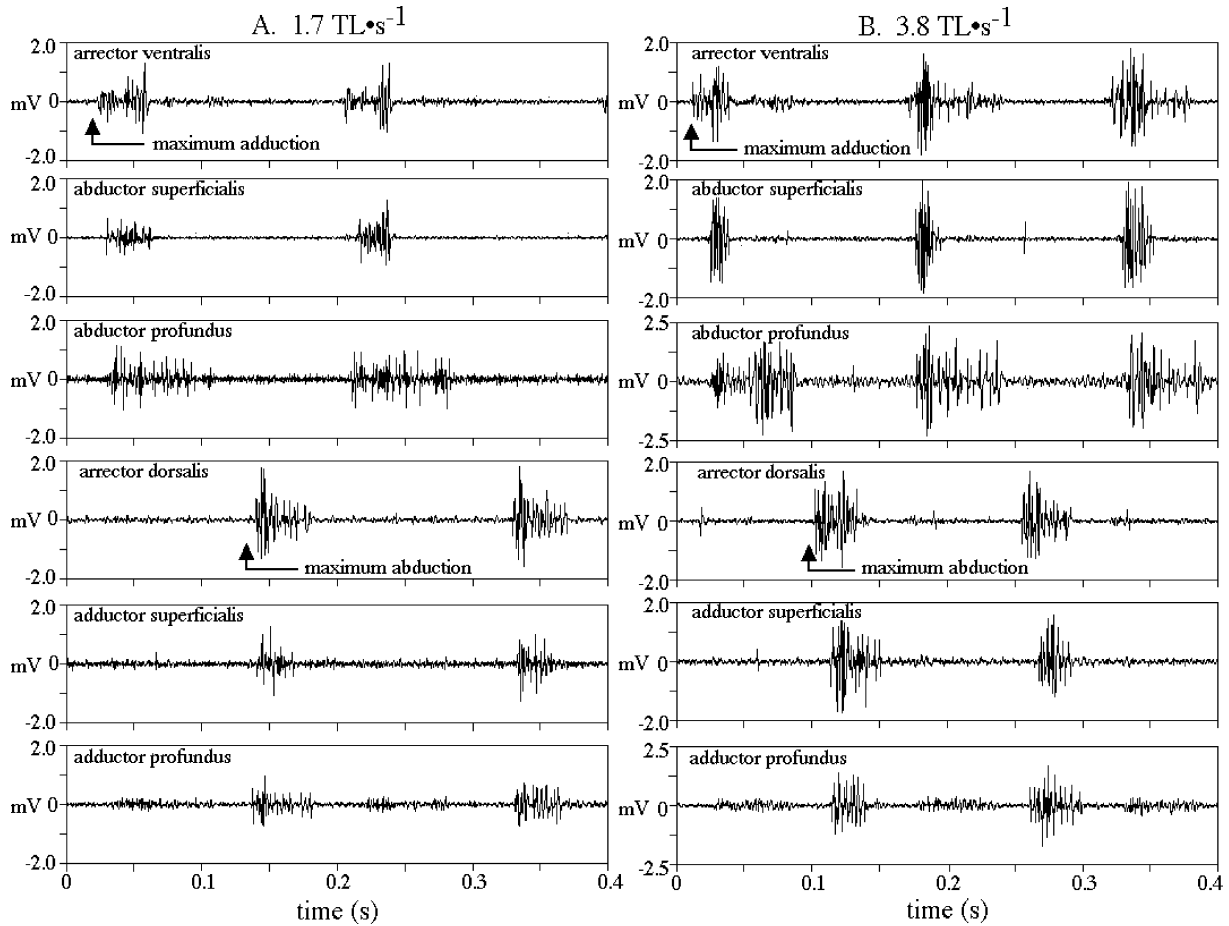


Fig. 31. Electromyograms [134] for six pectoral muscles at a speed of 1.7 (left) and 3.8 (right) body lengths/s. The time events correlate with kinematic landmarks in Fig. 30.

oscillatory in nature, the mean is nonzero, and the mean and instantaneous values are coupled. Little progress has been made on the control of such nonlinear systems with periodic or almost-periodic control inputs although they are common in swimming and flying animals [1], [57] and [129].

The ONR Biorobotics Program is attempting to build an engineering control device for precision maneuvering that consists of several integrated subsystems. An understanding of how the mechanical and neural architecture of pectoral fins are integrated is necessary for engineering success. This area is least developed and is reviewed here. More detailed reviews commissioned by ONR appear elsewhere [44]–[49].

A preliminary understanding of pectoral fin kinematics and function follows. Labriform is a mode of fish swimming characterized by the use of pectoral fins, rather than caudal, anal, or dorsal fins, and where whole body undulation is largely absent [130], [131]. Pectoral fins are lift- and acceleration-reaction-based and not drag-based devices. They operate in rowing or flapping mode. In rowing, the fin moves fore and aft. In flapping, the fin moves up and down. The leading edge has a variable twist along span during these motions. They use two sets of muscles, three in each set, to control leading-edge twist during these motions [108], [132]. There is now a convergence in the answer to the question: To row, or to flap? Flapping maximizes energy efficiency and is preferred for cruise at low speeds. However, to maneuver, rowing is preferable [133].

The detailed 3-D time-dependent topology (angle of attack and camber) of the pectoral fin of a live fish, in correlation to a

particular fish maneuvering motion, has not yet been measured. In the absence of that, the validity of even those computational fluid dynamic tools that can compute separated flows accurately is qualitative. One alternative would be to use a fluid-structure coupled code, and allow it to self-iterate the topology for a given station-keeping flow speed. How AMs can be woven to produce such dynamic topology needs to be addressed. The musculoskeletal morphology of pectoral fins and its mechanical analog are shown in Fig. 29 [134]. The latter could have value in kinematic bench studies for engineering replication of pectoral fins.

Fig. 30 shows the time sequence of the pectoral fins of a fish carrying out station keeping motion and the corresponding muscle activities are shown in Fig. 31. The EMG signal in Fig. 31 indicates that the abductor (downstroke) and adductor (upstroke) muscles act alternately. The superficialis and profundus operate simultaneously. The arrector dorsalis leads adductor pairs. The EMG durations do not change significantly when speed is doubled. The EMG characteristics are also not universal between species. It is unknown what the best model of animal with pectoral fin is for AUV application. Sunfish [38] is a candidate because it uses only pectoral fins for station keeping. Once the basic biology-based pectoral fin composed of AM is operational, it would be optimized for AUV application independent of further input from biology.

Most engineering control experience is based on linear behavior. Actuators can be assembled into independently controlled bundles acting in parallel. This would mimic, to

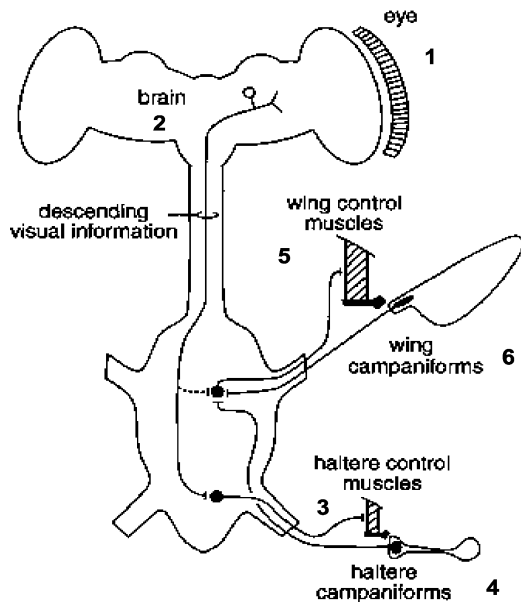


Fig. 32. Vision to wing-beat control hypothesis in fly flight [135] follows the path 1–6, via the coriolis force sensing organ called haltere (gyroscope).

the basic order, the organization of muscle control into independent motor units. Advanced electromechanical analogs [134], beyond the one shown in Fig. 29 that simulate the motor pattern of the muscoskeletal fin system, would help distill the neuro-physiology for engineering implementation.

#### A. Engineering Analogs of Biological Sensory-Motor Control

Aquatic animals, via coordinated activities of sets of muscles, produce a repertoire of motions (called primitives). The goal is to understand the sensory-motor control of similar primitives for AUV application (A similar approach for flying platforms has been made). The flight-control mechanism of fruit flies may be a model of the role of sensory feedback in motion control [45], [135]. Flies have an organ, called haltere. It is an active sensory organ sensitive to coriolis forces and is critical in stabilizing the platform during flight. As per the hypothesis depicted in Fig. 32, the visual system actively manipulates the reflex loop of haltere equilibrium. The incoming visual information activates the haltere-control muscles (bottom-hatched box) to alter the haltere kinematics during flight. The consequence of the change in haltere beating is to activate the haltere campaniform neurons, which then feed forward to the wing-steering muscle groups (upper hatched box). Thus, it is through the haltere system that vision controls the motoneurons of the wings (path 1-2-3-4-5-6).

Animal muscles that are active control actuators display a nonlinear stress versus elongation behavior [136]. For example, they could increasingly stiffen with increasing deflection. Such passive mechanical properties could stabilize a pectoral fin during phases when high deflection is required. The maneuvering motion of an AUV can be looked as one built by sequencing several elementary modules (primitives) of motion. Figs. 33 and 34 are examples of the physiological basis for hierarchical organization in the motor system [137], [138].

Engineering implementation of these biological approaches to the control of platform motion is a challenging area. An interaction between the artificial muscle and the neuro-physiology-

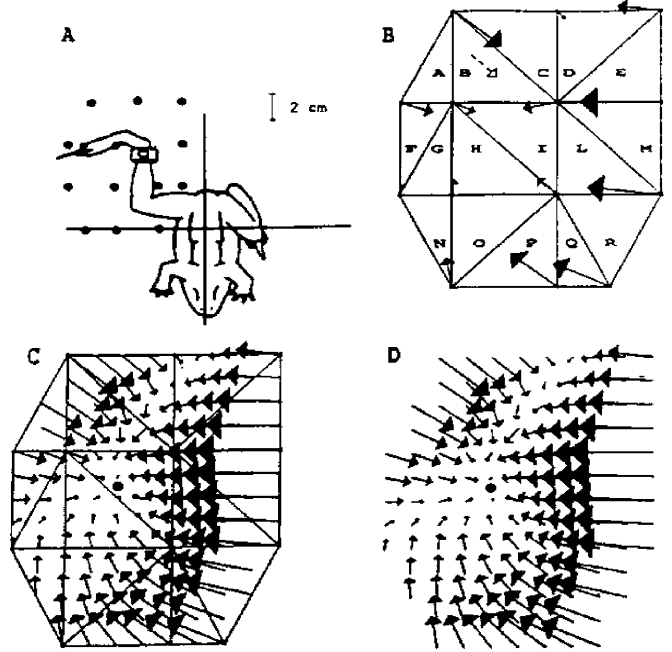


Fig. 33. Electrical stimulation of a site in the lumbar spinal cord of a vertebrate (A) induces the activation of multiple muscles [137]. This activity results in a pattern of forces (B) across a limb's workspace, which can be characterized as a smooth force field (C and D).

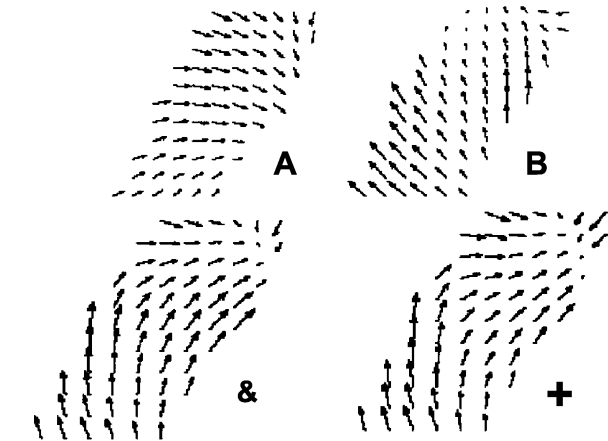


Fig. 34. Force fields generated by two spinal modules add linearly. In this experiment, field A and B were generated by stimulating two separate sides [138]. Field marked & was induced by the simultaneous activation of both sides. Field marked + is the vector sum of A and B. This illustrates how motor synergies may be combined to create more complex patterns of control.

based control groups would result in a pectoral fin device that would allow an AUV to self-regulate in the energetic environment of littoral zone.

#### B. Viability

Two approaches to control of platform motion could be considered. One is based on an assembly of motion primitives as discussed previously. This has been explored in flying vehicles but not in water borne vehicles. The other is based on neuroscience.

The present approach to the design of a control surface for a platform is a departure because of the presence of dynamic foils, unproven materials, and control technologies. The following is

TABLE VIII  
RATIONALE FOR ANALOG-DIGITAL HYBRID SYSTEM FOR IMPLEMENTATION OF NEUROSCIENCE-BASED ACTUATOR-SENSOR CONTROL

|   | Engineering  |   | Nature   |
|---|--|---|--|
| Principle   | Digital Technology   | Analog Technology   | Neural Networks  |
| Energy consumption  | High due to high clock rates keeping parts always powered for action.  | Several orders of magnitude less power consumption; takes up less space on silicon.   | Consumes very low power and takes up very little space   |
| Memory  | Reliable non-volatile memory exists.   | Highly reliable non-volatile memory needs more development.   | Synoptic strength is equivalent to memory  |
| Interfacing with sensor/actuator  | Requires extra components such as A/D and D/A converters and filters for signal processing and anti-aliasing. A drawback is the dependency on sampling rate which could be too high and expensive.   | Easy interface with real world, but design is hard due to difficulties in accurate noise computation. Signal conditioning is more difficult to get right in case of a significant mismatch in the characteristics of the signals (sensor/actuator signals and signals related to the computation). If signals are matched already then no extra components are needed. Furthermore, there is no sampling rate limitation. | Amenable to easy interface because signal characteristics of brain signals and sensor/actuator signals are matched.  |
| Design for noise  | Design is not a problem; more bits give higher precision encoding.   | Less practical ways of eliminating noise. Analog noise filters are possible.  | Robust with respect to noise due to redundancy and parallelism.  |
| Impact on performance   | Deteriorates with increasing noise.  | Deteriorates with increasing noise  | Performance improves with noise via models such as noisy threshold, reset or integration.  |
| Maturity  | Highly reliable and matured; scalable  | Older than digital; however, less matured; quality control has room for improvement; advantages are fast, reliable and cheap computation and interfacing  | Engineering system implementation not yet matured. Hybrid (analog-digital) approach has potential; continuous hardware can greatly enhance speed because each time slice does not need to be iterated; amenable to VLSI system implementation; highly scalable |
| Hybrid Analog-Digital System for Implementation of Neuroscience-Based Control | The most likely implementation of efficient neuroscience-based control design will be one based on both analog and digital hardware technologies. The analog hardware will be utilized to build the computational framework and reproduce as closely as possible the nature of the structure (i.e., massive connectivity, parallelism, redundancy) and the signal characteristics (spiking, analog asynchronous signals) of the natural brain. The digital hardware will be used to effectively implement brain-sensorimotor communication and non-volatile storage. |   |  |

a list of viability issues [139]. The risks inherent to dynamic control surfaces are reliability and cost. Insurance would be the system-based optimized design at molecular level, as mentioned in the section on artificial muscle actuator technology. Interaction between pitch, heave, and twist of foils could complicate the approach to control. A typical pectoral fin is composed of six muscles. Three of them control the leading edge deflections and the others control the trailing edge motion. Within the actuator muscle structure, friction between such layers, the substrate and electrodes could affect performance. When biological muscles move, they change their stiffness and damping properties. The controllability of the impedance properties is unknown.

While linear behavior is better understood, nonlinear behavior offers advantages. Some nonlinear mechanical properties are believed to play an important role in motion control. For example, muscle viscous behavior can depend on a fractional power of limb velocity. This has been suggested to play a role in the termination of movement without oscillations. Another question is regarding the impact of hysteresis on control: How important is it to avoid or to reduce it? The role of muscle redundancy in control is not obvious. Biological systems are characterized by an apparent “excess” of control muscles at each degree of freedom. In addition, the biological design of muscles is based on multiple independently controlled compartments (the motor units) operating in parallel. Should artificial muscle design follow the same approach? If so, how

should multiple compartments be controlled? It is unclear how the functional synergy observed in biological muscle systems should be modeled in an engineering control. In a system with multiple degrees of freedom, synergies may be defined as sets of muscle elements that are simultaneously activated and that establish some specific couplings. Then, synergies may be considered as independent actuators. How should synergies be designed given a repertoire of desired behaviors? Control factors specific to AUVs compared with ground or avian platforms are the following: Damping because of viscosity, added mass of water, and buoyancy.

Neural structures are deemed to be better suited for unstructured environments. Therefore, an approach based on a combination of motion primitives and neural structures could yield very versatile control. Information processing in biological systems has now reached a level of maturity where they are more amenable to engineering implementation. Table VIII shows the rationale for a hybrid analog-digital system for implementing neuroscience based control [150].

## VI. INTEGRATION OF BIOLOGY-BASED HYDRODYNAMICS, ACTUATORS AND CONTROL IN AUV

### A. Viability

Navy propulsors and platforms have been developed at system level over many years. The former has reached a high-

TABLE IX  
ESTIMATION OF POWER FOR BIOROBOTIC AUV IN TABLE VI [3], [116]

| Vehicle identification | Vehicle size                 | Vehicle speed | Tail propulsion fin frequency | Motor cycles | Fuel     | Power                                       |
|------------------------|------------------------------|---------------|-------------------------------|--------------|----------|---|
| Baseline               | 0.53 m diameter x 5.3 m long |               | Not applicable                |              |          | 50 W  |
| Low-speed (Table VI)   | 0.53 m diameter x 5.3 m long | 1.8 m/s       | 3 Hz                          | 1.7 M        | 100 0 km | 64 W (current technology)                   |
| High-Speed (Table VI)  | 0.53 m diameter x 5.3 m long | 7.5 m/s       | 12 Hz                         | 0.32 M       | 200 km   | 48 kW (current technology, projected power) |

propulsive efficiency and operationally the system has proven to be rugged. Biology-inspired systems have potential to be implemented on platform systems if they offer new capability in adaptability, nonlinear control or performance in off-design (off-cruise) condition, such as low-speed maneuverability, where efficiency is not always of prime concern. NUWC measurements of flapping foils attached to rigid cylinders indicate an efficiency that is half of that resulting from conventional propulsors attached to a cylinder [65]. Similar reductions have been observed for engineering implementation of pectoral fins also [140]. These foils oscillate like caudal fins of fish and do not simultaneously heave and pitch. The following question arises: What are the sources of penalty in the engineering implementation of idealized biology-based mechanisms? A quantitative accounting of the penalties and comparison with a conventional engineering system would be instructive.

A comparative study of existing artificial muscle technologies has been conducted to determine which ones could meet the hydrodynamic criterion in Table VI. The problem definition is given in Table IX [3], [116].

Fig. 35 presents an estimated comparative assessment of various artificial muscles that meet the requirements in Table IX. Most of them can meet the low-speed (3.6 kts) criterion. Only one of the conducting polymer technologies is anticipated to meet the criterion at the higher speed of 15 kts. Considering the muscle-like properties of CEAP, a relatively rational approach to the molecular design and the property milestones reached so far, an effort into its development is underway [151].

## VII. BIOROBOTIC VEHICLES: CURRENT AND FUTURE

Several underwater biorobotic platforms of exploratory nature are discussed. They fall in two categories depending on the fish fin they emulate: those having one or more flapping foils similar to the caudal fins of fish; and those incorporating simultaneously heaving and pitching mechanical pectoral fins. Since

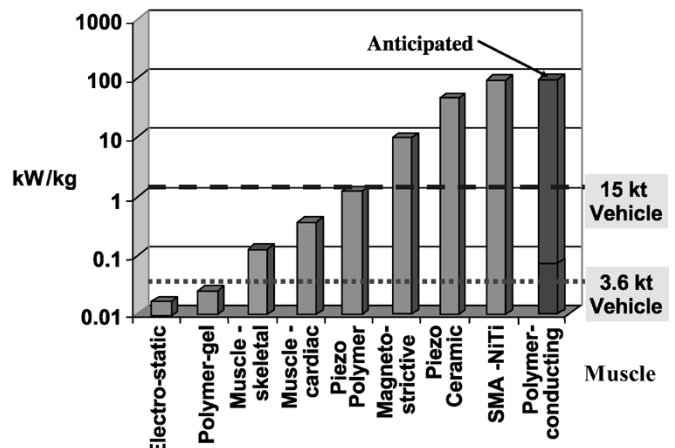


Fig. 35. Comparative assessment [3], [116] of artificial muscle-like actuator technologies in meeting the biorobotic AUV pectoral fin requirements given in Tables VI and VIII.



Fig. 36. NUWC bottom swimmer. The ruler is 30 cm (12") long.

biorobotic AUVs are currently seen as especially maneuverable platforms, the latter is gaining in prominence.

### A. Flapping Foil Vehicles

Figs. 36 and 37 show the NUWC Bottom Swimmer and the MIT Robopike. Notice that they mostly have a rigid hull. The NUWC platform has four pairs of flapping foils mounted in a cruciform, each controllable independently via digital means. Flapping foils produce high levels of peak forces that are also sinusoidal in amplitude with time. Thus, a cruciform arrangement would allow the production of high levels of force at all times. Any side-to-side oscillation of the head could also be prevented. The hull is the so-called B1 Body, which produces an accelerating followed by a decelerating boundary layer. For this reason, the enlarging part of the hull remains laminar even at high speeds in the contaminated (with plankton, for example) oceanic environment. This feature would permit the placement of sonar and visual devices because the absence of a propulsor would diminish the stirring of benthic sediments. In addition, since the tail end of the platform axis is nonrotating, the platform is amenable to the placement of towed cables. The MIT platform has one flapping foil attached to the tail.

Fig. 37 shows the MIT-Draper Robopike. Measurements at NUWC indicate that flapping foils attached to the tail of a rigid cylinder have an efficiency of about 40%, which is roughly half of that of an AUV. A similar reduction is found in pectoral fins attached to a rigid hull [140]. Flapping foils are not being considered to supplant any conventional propulsor. However, they

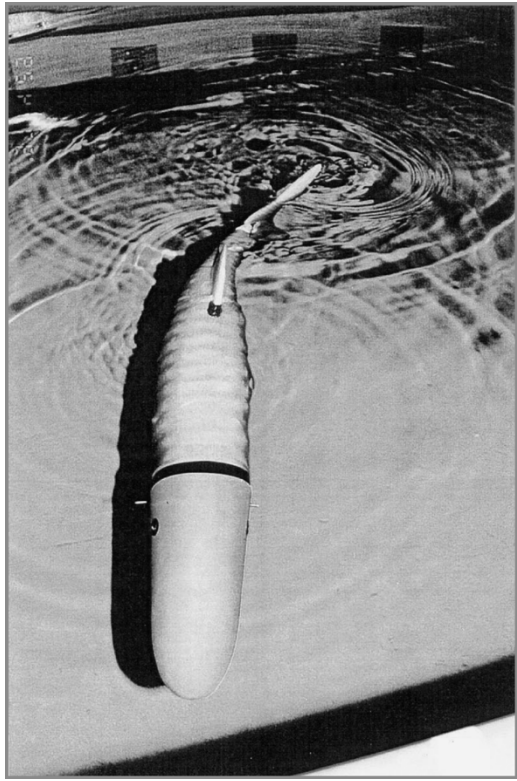


Fig. 37. MIT-Draper Robopike. Notice the rigid front half and a cylindrical shape of the hull.

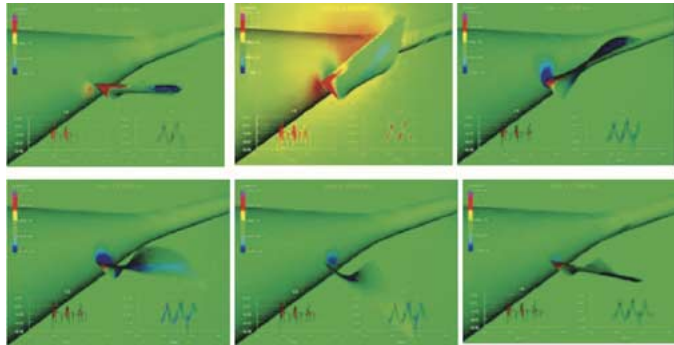


Fig. 38. Computational simulation [3], [141] of a 0.53 m diameter UUV propelled by a pair of wrasse-fish inspired pectoral fins mounted on its tail. The deflections of the fin, consisting of heave, pitch and twist, at different phases and the color coded pressure distributions on the fin surface are indicated. For time traces, see the caption of Fig. 18.

are of value in maneuvering because they produce high levels of transient force.

The route to potential transition of biorobotic devices is by retrofitting to existing rigid hull platforms and components like conventional propulsors. The hull platforms with flapping foil thrusters, as shown in Figs. 36 and 37, are radical and raise practical concerns. Instead, three retrofittable pectoral fin devices like those shown in Figs. 38–41 are in consideration for further development in concert with current efforts devoted to the Exploratory Development of AUVs. Fig. 38 shows a computational effort where two wrasse fish pectoral fin devices are attached to the tail end of a 21 in (0.53 m) diameter cylinder keeping its station (recall wrasse fish fin computations as shown

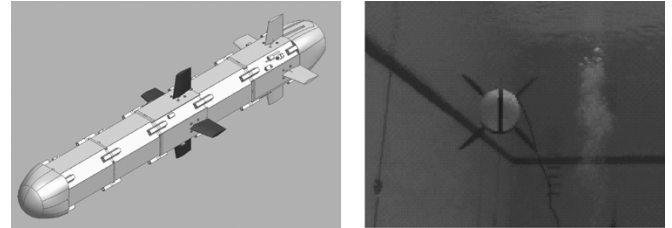


Fig. 39. Biology inspired “pectoral fins” for precision maneuvering of AUVs. The left figure shows a schematic of fins attached to a conventional AUV. The figure on right shows the Nekton Pilot Fish with four “pectoral fins” in a tank [58].

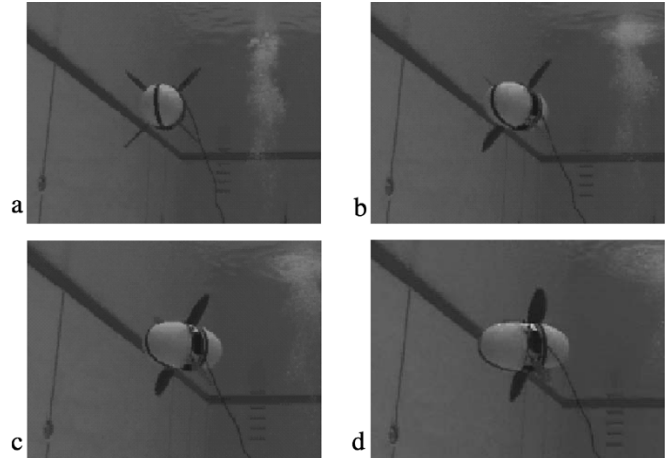


Fig. 40. Motion of Nekton Pilot Fish [58] shown in Fig. 39 (right). Notice that the hull is turning toward the vertical wire on left.

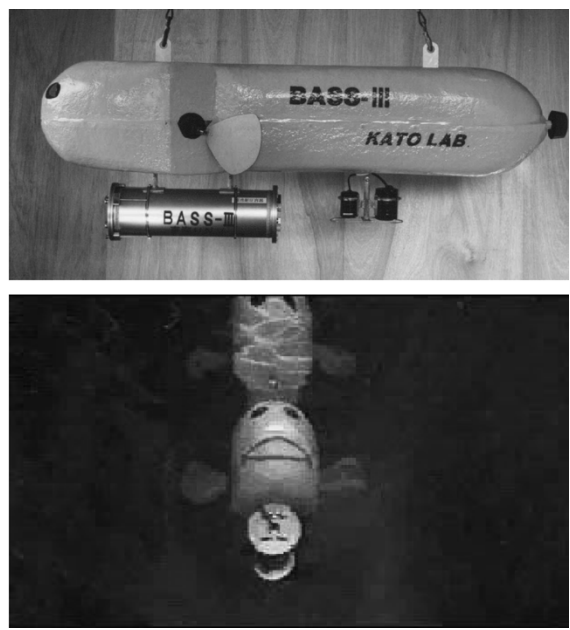


Fig. 41. Rigid cylindrical hull AUV with a pair of “pseudo-pectoral” fins. The U.S.-Japan model is similar [142], [144]. The top figure shows a side view, while the bottom figure shows a head on view of the vehicle in a tank.

in Fig. 18 [107]). The parameters for scaling up the fin from fish to the AUV are shown in Table X. These preliminary computations suggest that two reasonably sized biorobotic pectoral fins would permit the 0.53-m diameter vehicle to keep station at a stream speed of 5 kts.

TABLE X  
COMPUTED PARAMETERS OF A WRASSE FISH FIN AND THEIR SCALING FOR AUV APPLICATION SHOWN IN FIG. 38 [3], [141]

|  | <i>Wrassie fin</i>       | <i>UUU fin</i>          |
|--|--------------------------|-------------------------|
| <i>Leading edge length</i>   | 3.5 cm                   | 19.84 cm                |
| <i>Trailing edge length</i>  | 1.5 cm                   | 8.55 cm                 |
| <i>Area</i>  | 4.63 cm <sup>2</sup>     | 140.7 cm <sup>2</sup>   |
| <i>Body area</i>   | 176.32 cm <sup>2</sup>   | 92024 cm <sup>2</sup>   |
| <i>Stream velocity for station keeping</i>                             | 45 cm/s                  | 257.4 cm/s              |
| <i>Flow speed at foil tip at foil oscillation frequency of 3.33 Hz</i> | 50 cm/s                  | 290 cm/s                |
| <i>Pressure minimum (gage)</i>   | -4.95x10 <sup>4</sup> Pa | -7.2x10 <sup>4</sup> Pa |
| <i>Pressure maximum (gage)</i>   | 2.68x10 <sup>4</sup> Pa  | 6.6x10 <sup>4</sup> Pa  |

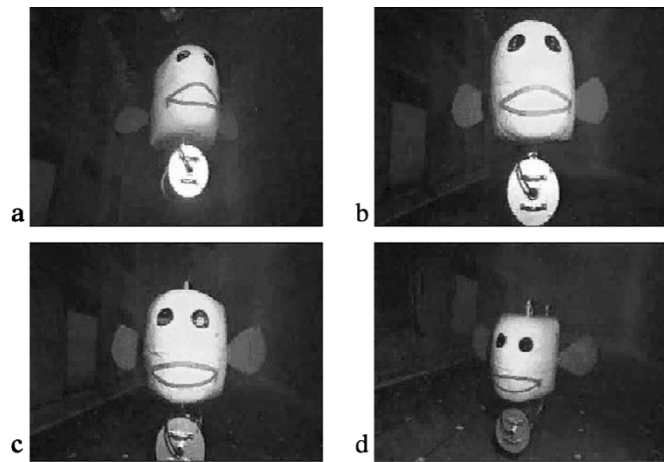


Fig. 42. Maneuvering motion of vehicle in Fig. 41 [144]. Notice that the hull is moving looking left to right while also moving forward and toward the bottom.

### B. "Pectoral Fin" Vehicles

Figs. 39 and 40 show the Nektor pectoral fin device [58]. Figs. 41 and 42 show the ONR-sponsored U.S.-Japan pectoral fin device [142]–[144]. Their approach to precision docking in test tanks is shown. These fins are rigid and do not replicate all degrees of motion of a live fin. They are powered by conventional motors. These two pectoral fin-based AUVs are compared in Table XI.

On closer inspection, Figs. 41 and 42 actually show the pectoral fins as simply rigid surfaces attached to a rigid hull but in the pectoral area. Although they have been labeled as pectoral fins [143], in the early versions, they actually performed as caudal fins that are merely attached in the pectoral region of the hull (flapping back and forth, or up and down, or simply oscillating about its axis). They do not appear to have the high-lift mechanism that comes from simultaneous heave and pitch in a figure-of-eight motion. For this reason, they have been termed "pseudo-pectoral" fins in Fig. 41. However, in later designs, the performance of rigid Nektor pectoral fins has been improved by flexible fins where heaving motion is simulated by dint of resonant fins made of polyurethane, which is a soft material, but with restriction of operation only at 6 Hz and an aspect ratio of 1.0 [156]. The understanding of high-lift mechanism in pectoral fins in underwater swimming is not advanced as it is in the flight of fruit flies [93], [94], and [153]. Fig. 43 shows the NUWC

TABLE XI  
COMPARISON OF ONR-SPONSORED "PECTORAL-FIN" BASED AUVs

| Investigators                 | [58 & 140]   | [142]  | [154, 155]  |
|-------------------------------|--|--|---|
| <i>AUV Name</i>               | Pilot Fish (150 Kg)  | BASS: US-Japan   | NUWC BAUV   |
| <i>Bio-Inspiration</i>        | Black Bass Pectoral Fin Based  | Pectoral Fin Based   | Pectoral Fin Based  |
| <i>Fin motion</i>             | Pitch and/or Heave   | Pitch or Heave   | Pitch and Heave   |
| <i>Number of fins</i>         | 4 Fins in x-form   | 2 Fins   | 3 + 3 Fins  |
| <i>Fin Rate</i>               | 2 – 4 Hz Continuous; 20 Hz Burst   | 3 Hz Continuous  | 0.5 – 1.5 Hz Continuous and Burst   |
| <i>Diameter x length</i>      | 50 cm  | 10 cm x 120 cm   | 20 cm x 160 cm  |
| <i>Fin: span x chord (cm)</i> | 40 x 20 Elliptical planform NACA 0014  | 8.3 x 10   | 15 x 7.5 Modified NACA 0012-64  |
| <i>Fin Drive</i>              | Four 2.5 kW direct drive servomotors   | 3 Motors for each fin  | 2 Servos for each fin   |
| <i>Efficiency (Bollard)</i>   | 0.4, Half that of comparable propellers  |  | > Cross Tunnel Thruster Efficiency  |
| <i>Maneuverability</i>        | 0.6 to 0.0 m/s in 12 cm; Turn rate: > 150 deg/s; Angular acceleration: > 800 deg/s <sup>2</sup> ; Burst acceleration: > 0.4g | Forward & Backward: ascend & Descend; small radii turn; lateral swim | On surface & underwater, 6 degrees of freedom, forward & backward, small radii turns, sway, station keeping |
| <i>Navy Transition</i>        | Florida Atlantic University Morpheus AUV   | None   | Supplanting Cross Tunnel Thrusters  |

biorobotic autonomous vehicle as of March 2005, which can swim both underwater and on surface. The vehicle has six foils, each of which can independently undergo a simultaneous heave and pitch motion. This vehicle has been built to supplant the so-called cross tunnel thrusters (CTTs) for hovering. Hydrodynamic measurements show that, in hover mode, these actuators consume half the hydrodynamic power (W) to produce the same amount of vertical lift force (N) of a pair of CTTs [154]. Power saving is indicated over the Nektor actuators as well when in motion [155].

### VIII. IMPACT ON RADIATED NOISE OF UNDERWATER VEHICLES

In underwater vehicles, the main source of radiated noise is hull vibration transmitted from the drive train, namely the motors, gears, and shafting of the propulsor. Ideally, an artificial muscle actuator would supplant such drives and offer unprecedented quietness [127], [128]. The other source of noise is the propulsor. It is unclear if pectoral fin devices would be a source of cavitation noise because of their reliance on vortex flows. Apart from cavitation, a conventional propulsor has three other sources of noise: Blade rate tonals resulting from upstream wake deficit; trailing edge singing from vortex shedding; and the effect of turbulence ingested from upstream hull. All three sources of noise are approximately described by power laws

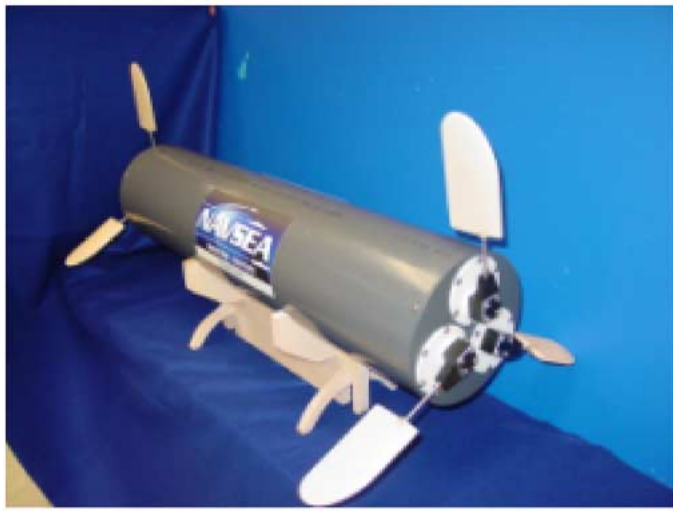


Fig. 43. NUWC biorobotic autonomous underwater vehicle.

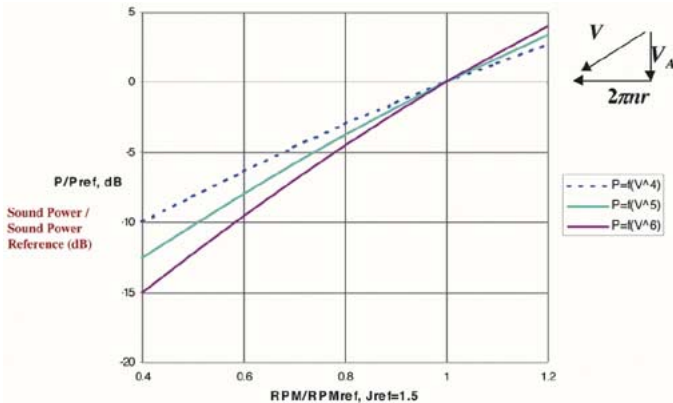


Fig. 44. Modeling of the effects of RPM reduction on radiated noise of traditional propulsors [3], [127]. Advanced coefficient  $J = V_A/(nD)$ , where  $V_A$  is speed of advance ( $m/s$ ),  $n$  = shaft speed ( $rotations/s$ ) and  $D$  = maximum propeller diameter ( $m$ ).

of rotational rates of 4, 5, and 6, respectively. A theoretical modeling was carried out to determine the reduction in radiated noise because of a reduction in RPM [3], [127], and [145]. This is shown in Fig. 44. A 10% reduction in RPM can lead to a reduction of 3–5 dB, which is measurable. Thus, a reduction in RPM should be sought via enhanced lift while forward speed remains unchanged. This NUWC strategy is being implemented on a small propulsor in a passive manner [59]. However, only the leading-edge dynamic stall mechanism is considered. The pitch of the upstream stator blades is varied azimuthally whereby a downstream rotor blade undergoes leading edge dynamic stall. Diametrically opposite stator blades are pitched oppositely whereby their far-field noise is cancelled. Notice that while conventional propulsor design strives to feed a uniform flow to the rotor, this passive approach contrives a periodic inflow to the rotor to generate high-lift. Cavitation and drag penalties are unknown. Preliminary analysis indicates an RPM and noise reduction of 35% and 3 dB, respectively.

In the low-speed range, if pectoral fin propulsors supplant conventional propulsors, then the noise spectrum could be drastically altered as shown by the dotted lines in Fig. 45. A pectoral

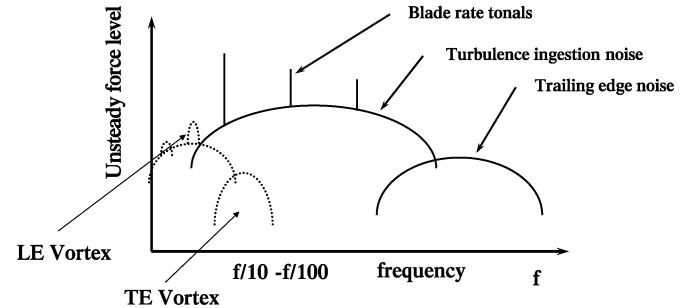


Fig. 45. Schematic summary [3], [127] of noise sources for traditional propellers (solid lines on right) compared with speculative improvements in radiated noise spectra due to pectoral fin thrusters (broken lines on left) in arbitrary scale.

fin does not rotate about the vehicle axis but rather rotates about its own axis and at RPMs generally well below that of a conventional propulsor. The operating frequencies would be one-tenth of that of a current propulsor, and blade tonals would be absent resulting from the absence of stators. Because of the presence of unsteady lifting mechanisms, ingested turbulence would have no effect. Foil-trailing edge singing would still be present although at lower frequencies. The vehicle wake swirl could be weaker because the foils do not rotate around the vehicle axis. However, new sources of noise would be present because of the buffeting of foils by unsteady leading and trailing edge vortices. While this is speculative, differences in the noise spectrum seem reasonable even after penalties are paid.

## IX. CONCLUDING REMARKS

This paper has discussed the progress in building the scientific foundation of underwater biorobotic AUVs and their engineering implementation. This area of research has been growing rapidly over the last decade [146]–[148], [153]. A discovery and two milestones have spurred a bright outlook. Steady-state mechanisms, on which current engineering lifting surfaces are built, do not explain how fruit flies fly; it is now understood that they resort to unsteady aerodynamic mechanisms to produce the required high lift [89], [93]. It is important to realize that the implementation of these seemingly complicated dynamic mechanisms in a complete platform system is feasible. The implementation of such mechanisms prevalent in the biological world on an engineering platform would require the development of artificial muscles for control actuators and the engineering simulation of their neuroscience-based control. These milestones, in principle, have now been reached. Electro-active polymers now have been developed in a laboratory environment that matches the properties of mammalian muscles [121] although we need to go further ( $\times 10 \times 100$ ) to meet engineering needs. Live neurons have also been used to drive a laboratory mechanical robot indicating the progress in the viability of biology-based subsystems in the context of conventional engineering systems [149]. Neuroscience-based controllers have been built and are being tested in engineering platforms in NUWC [47].

The thrust of the current ONR Biorobotics Program is on the implementation of the biology-based science and technology on AUVs to enhance their low-speed maneuvering capabilities, which include the following: hovering, small-radius turning,

rising, sinking, and precision station keeping. The AUV implementation of biorobotics so far has made use of only the hydrodynamics of aquatic animal-inspired control surfaces. Even in that, the degree-of-freedom of the control surfaces remains limited when compared with that occurring in the animal world, thereby limiting their performance. A significant leap would be the construction of such control surfaces with appropriate artificial muscles while incorporating a neuroscience-based control. Currently, the hydrodynamics component is the most developed, although many issues regarding the mechanism at higher Reynolds numbers and generation of design-relevant data remain to be addressed. The artificial muscle component is the most critical technology for success but the promise of a useful product is yet to be realized. The neuroscience-based control aspects are the least developed and the potential of artificial muscle technology can be realized if this segment makes practical progress. For example, the superiority of neuroscience based control over conventional engineering needs to be demonstrated. These three disciplines need to be integrated and their development planned in a unified manner [3], [153].

The long-term broad goal of the program is to merge the above biorobotic AUV platform with biosonar and create a functionally equivalent dolphin. The broad operational motivation is the elimination of personnel from the littoral mine clearance loop and make the process fully mechanical.

#### ACKNOWLEDGMENT

The author would like to thank Dr. T. McMullen of ONR for sponsoring his biorobotics research at NUWC, Drs. T. Swean and T. Curtin of ONR for their helpful discussions, and Profs. M. Cutkoski of Stanford University and M. Dickinson and R. Fearing of the University of California, Berkeley for their valuable assistance. He would also like to thank Prof. F. Fish of Westchester University, Dr. J. Madden of MIT, and Prof. S. Mussa-Ivaldi of Northwestern University. The contributions of many others, including Dr. A. Menozzi of NUWC, Profs. L. Rome of the University of Pennsylvania, M. Triantafyllou of MIT, J. Walker of the University of Southern Maine, and Dr. M. Westneat of Chicago Field Museum, are appreciated.

#### REFERENCES

- [1] P. R. Bandyopadhyay, "Maneuvering hydrodynamics of fish and small underwater vehicles," *J. Integ. Comp. Biol.*, vol. 42, no. 1, pp. 102–117, 2002.
- [2] P. R. Bandyopadhyay, J. M. Castano, W. H. Nedderman, W. Krol, J. Raposa, and M. Mojarrad, Biomimetics Research at NUWC: 2000, Naval Undersea Warfare Center, Newport, RI, 2000.
- [3] *Proc. Office of Naval Research Pre-Workshop on High-Lift Biorobotics*, Arlington, VA, Jan. 29, 2002, (80 vugraphs), internal document.
- [4] D. R. Blidberg, *The Development of Autonomous Underwater Vehicles (AUVs): A Brief History*. Seoul, Korea: in AUSI ICRA, 2001.
- [5] T. B. Curtin and J. G. Bellingham, "Guest editorial: Autonomous ocean-sampling networks," *IEEE J. Ocean Eng.*, vol. 26, no. 4, pp. 421–423, Oct. 2001.
- [6] R. Gisiner, J. Tague, and P. Moore, ONR Biosonar Program Review, SPAWAR Systems Center, San Diego, CA, Aug. 13–14, 2002.
- [7] A. Rudolf, "DARPA DSO Controlled Biological Systems Program," unpublished, 2002.
- [8] M. Cutkoski, private communication, 2002.
- [9] R. S. Fearing, private communication, 2002.
- [10] R. J. Full and C. T. Farley, "Musculoskeletal dynamics in rhythmic systems—a comparative approach to legged locomotion," in *Biomechanics and Neural Control of Posture and Movement*, J. M. Winters and P. E. Crago, Eds. New York: Springer-Verlag, 2000.
- [11] M. Garcia, A. Kuo, A. M. Peattie, P. C. Wang, and R. J. Full, "Damping and size: insights and biological inspiration," in *Proc. Int. Symp. Adaptive Motion of Animals and Machines*, Montreal, QC, Canada, Aug., 8–12 2000.
- [12] J. G. Cham, S. E. Bailey, J. C. Clark, R. J. Full, and M. R. Cutkosky, "Fast and robust: Hexapedal robots via shape deposition manufacturing," *Int. J. Robot. Res.*, vol. 21, no. 10–11, pp. 869–882, 2002.
- [13] R. J. Full and D. E. Koditschek, "Templates and anchors—neuromechanical hypotheses of legged locomotion on land," *J. Exp. Biol.*, vol. 202, pp. 3325–3332, 1999.
- [14] N. G. Hatsopoulos, "Coupling the neural and physical dynamics in rhythmic movements," *Neural Comput.*, vol. 8, pp. 567–581, 1996.
- [15] J. K. Karpick, J. G. Cham, J. E. Clark, and M. R. Cutkosky, "Stride period adaptation for a biomimetic running hexapod," presented at the 10th Int. Symp. Robotics Research, Victoria, Australia, Nov. 9–12, 2001.
- [16] J. M. Camhi and E. N. Johnson, "High-frequency steering maneuvers mediated by tactile cues: Antennal wall-following in the cockroach," *J. Exp. Biol.*, vol. 202, pp. 631–643, 1999.
- [17] D. Schalle, "Antennal sensory system of *periplaneta americana*," *Cell Tissue Res.*, vol. 191, pp. 121–139, 1978.
- [18] K. Autumn, Y. A. Liang, S. T. Hsieh, W. Zesch, W. P. Chan, T. W. Kenny, R. Fearing, and R. J. Full, "Adhesive force of a single Gecko foot-hair," *Nature*, vol. 405, pp. 681–685, 2000.
- [19] O. Sotavalta, "The wing stroke frequency of insects in wing mutilation and loading experiments at sub-atmospheric pressure," *Ann. Zool. Soc.*, vol. 15, no. 2, pp. 1–67, 1952.
- [20] R. S. Fearing, K. H. Chiang, M. Dickinson, D. L. Pick, M. Sitti, and J. Yan, "Wing transmission for a micromechanical flying insect," in *Proc. IEEE Int. Conf. Robotics and Automation*, Apr., 24–28 2000, pp. 1509–1516.
- [21] M. Sitti, D. Campolo, J. Yan, R. S. Fearing, T. Su, D. Taylor, and T. Sands, "Development of PZT and PZN-PT based unimorph actuators for micromechanical flapping mechanisms," in *Proc. IEEE Int. Conf. Robotics and Automation*, Seoul, Korea, May 21–26, 2001, pp. 3839–3846.
- [22] R. J. Wood and R. S. Fearing, "Flight force measurements for a micromechanical flying insect," presented at the IEEE IROS 2001, Maui, HI, Oct.–Nov. 29, 2001.
- [23] J. Yan, S. A. Avadhanula, J. Birch, M. H. Dickinson, M. Sitti, T. Su, and R. S. Fearing, "Wing transmission for a micromechanical flying insect," *J. Micromech.*, vol. 1, no. 3, pp. 221–238, 2002.
- [24] M. H. Dickinson, F. Lehmann, and S. P. Sane, "Wing rotation and the aerodynamic basis of insect flight," *Science*, vol. 284, pp. 1954–1960, 1999.
- [25] S. P. Sane and M. H. Dickinson, "The control of flight force by a flapping wing: lift and drag production," *J. Exp. Biol.*, vol. 204, no. 19, p. 3401, 2001.
- [26] W. Nachtigall, A. Wisser, and D. Eisinger, "Flight of the honey bee. VIII. Functional elements and mechanics of the "Flight Motor" and the wing joint—one of the most complicated gear-mechanisms in the animal kingdom," *J. Comp. Physiol. B*, vol. 168, no. 5, pp. 323–344, 1998.
- [27] S. Avadhanula, R. J. Wood, D. Campolo, and R. S. Fearing, "Dynamically tuned design of the MFI thorax," presented at the IEEE Int. Conf. Robotics and Automation, Washington, DC, May 11–15, 2002.
- [28] J. Yan, R. Wood, S. Avadhanula, M. Sitti, and R. S. Fearing, "Toward flapping wing control for a micromechanical flying insect," in *Proc. IEEE Int. Conf. Robotics and Automation*, Seoul, Korea, May 21–26, 2001, pp. 3901–3908.
- [29] L. F. Tammero and M. H. Dickinson, "The influence of visual landscape on the free flight behavior of the fruit fly *drosophila melanogaster*," *J. Exp. Biol.*, vol. 205, no. 3, pp. 327–343, 2002.
- [30] W. C. Wu, R. J. Wood, and R. S. Fearing, "Halteres for the micromechanical flying insect," presented at the IEEE Int. Conf. Robotics and Automation, Washington, DC, May 11–15, 2002.
- [31] L. Schenato, W. C. Wu, and S. Sastry, "Attitude control for a micromechanical flying insect via sensor output feedback," in *Proc. 7th Int. Conf. Control, Automation, Robotic, and Vision*, Singapore, Dec. 2002, pp. 1031–1036.
- [32] ———, "Attitude control for a micromechanical flying insect via sensor output feedback," *IEEE Trans. Robot. Autom.*, vol. 20, no. 1, pp. 93–106, Feb. 2004.

- [33] W. C. Wu, L. Schenato, R. J. Wood, and R. S. Fearing, "Biomimetic sensor suite for flight control of a micromechanical flight insect: Design and experimental results," in *Proc. ICRA 2003*, Taipei, Taiwan, pp. 1146–1151.
- [34] R. S. Deng, L. Schenato, and S. S. Sastry, "Model identification and attitude control for a micromechanical flying insect including thorax and sensor models," in *Proc. ICRA 2003*, Taipei, Taiwan, pp. 1152–1157.
- [35] ———, "Hovering flight control of a micromechanical flying insect," presented at the IEEE Int. Conf. Decision and Control, Orlando, FL, Dec. 2001.
- [36] L. Schenato, X. Deng, and S. Sastry, "Flight control system for a micromechanical flying insect: Architecture and implementation," in *Proc. IEEE Int. Conf. Robotics and Automation*, Seoul, Korea, May 21–26, 2001, pp. 1641–1646.
- [37] E. Shimada, J. A. Thompson, J. Yan, R. J. Wood, and R. S. Fearing, "Prototyping millirobots using dexterous microassembly and folding," presented at the Symp. Microrobotics, ASME Int. Mech. Eng. Cong. and Exp., Orlando, FL, Nov. 5–10, 2000.
- [38] G. Lauder and E. G. Drucker, "Morphology and experimental hydrodynamics of fish fin control surfaces," *IEEE J. Ocean. Eng.*, vol. 29, no. 3, pp. 556–571, Jul. 2004.
- [39] P. W. Webb, "Maneuverability—definitions and general issues," *IEEE J. Ocean. Eng.*, vol. 29, no. 3, pp. 547–555, Jul. 2004.
- [40] M. S. Triantafyllou, A. H. Techet, and F. S. Hover, "Review of experimental work in biomimetic foils," *IEEE J. Ocean. Eng.*, vol. 29, no. 3, pp. 585–594, Jul. 2004.
- [41] R. Mittal, "Computational modeling in bio-hydrodynamics," *IEEE J. Ocean. Eng.*, vol. 29, no. 3, pp. 595–604, Jul. 2004.
- [42] J. A. Walker, "Kinematics and performance of maneuvering control surfaces in teleost fishes," *IEEE J. Ocean. Eng.*, vol. 29, no. 3, pp. 572–584, Jul. 2004.
- [43] F. E. Fish, "Structure and mechanics of nonpiscine control surfaces," *IEEE J. Ocean. Eng.*, vol. 29, no. 3, pp. 605–611, Jul. 2004.
- [44] F. A. Mussa-Ivaldi, "Physiology and neural control of pectoral fins of aquatic animals: Introduction and roadmap," presented at the 13th Int. Symp. Unmanned Untethered Submersible Technology, Durham, NH, Aug. 24–27, 2003.
- [45] F. A. Mussa-Ivaldi and S. A. Solla, "Neural-primitives for motion control," *IEEE J. Ocean. Eng.*, vol. 29, no. 3, pp. 640–650, Jul. 2004.
- [46] J. E. Colgate and K. M. Lynch, "Control problems solved by a fish's body and brain: A review," *IEEE J. Ocean. Eng.*, vol. 29, no. 3, pp. 660–673, Jul. 2004.
- [47] R. R. Llinas, E. Leznik, and V. I. Makarenko, "The Olivocerebellar as a universal motor control system," *IEEE J. Ocean. Eng.*, vol. 29, no. 3, pp. 631–639, Jul. 2004.
- [48] M. A. MacIver and J. W. Burdick, "Neuromechanical design and active sensory systems in animals," *IEEE J. Ocean. Eng.*, vol. 29, no. 3, pp. 651–659, Jul. 2004.
- [49] M. W. Westneat, D. H. Thorsen, J. A. Walker, and M. E. Hale, "Structure, function, and neural control of pectoral fins in fishes," *IEEE J. Ocean. Eng.*, vol. 29, no. 3, pp. 674–683, Jul. 2004.
- [50] J. D. Madden, N. Vandesteeg, P. G. Madden, A. Takshi, R. Zimet, P. A. Anquetil, S. Lafontaine, P. A. Wierenga, and I. W. Hunter, "Artificial muscle technology: Physical principles and naval prospects," *IEEE J. Ocean. Eng.*, vol. 29, no. 3, pp. 706–728, Jul. 2004.
- [51] P. G. Madden, J. D. Madden, P. A. Anquetil, N. A. Vandesteeg, and I. W. Hunter, "The relation of conducting polymer actuator material properties to performance," *IEEE J. Ocean. Eng.*, vol. 29, no. 3, pp. 696–705, Jul. 2004.
- [52] J. Paquette and K. J. Kim, "Ionomeric electro-active polymer artificial muscle for naval applications," *IEEE J. Ocean. Eng.*, vol. 29, no. 3, pp. 729–737, Jul. 2004.
- [53] A. M. King, D. S. Loiselle, and P. Kohl, "Force generation for locomotion of vertebrates: Skeletal muscle overview," *IEEE J. Ocean. Eng.*, vol. 29, no. 3, pp. 684–691, Jul. 2004.
- [54] P. R. Bandyopadhyay, J. M. Castano, J. Q. Rice, R. B. Philips, W. H. Nedderman, and W. K. Macy, "Low-speed maneuvering hydrodynamics of fish and small underwater vehicles," *ASME J. Fluids Eng.*, vol. 119, pp. 136–144, 1997.
- [55] P. R. Bandyopadhyay, "Brisk Maneuvering Device for Undersea Vehicles," U.S. Patent no. 5 939 665, Aug. 17, 1999.
- [56] P. R. Bandyopadhyay, W. H. Nedderman, and J. Dick, "Biologically inspired bodies under surface waves, part 1: load measurements," *ASME J. Fluids Eng.*, vol. 121, no. 2, pp. 469–478, 1999.
- [57] P. R. Bandyopadhyay, S. Singh, and F. Chockalingam, "Biologically inspired bodies under surface waves, part 2: Theoretical control of maneuvering," *ASME J. Fluids Eng.*, vol. 121, no. 2, pp. 479–487, 1999.
- [58] B. Hobson and C. Pell, private communication, 2002.
- [59] W. J. Usab Jr., A. J. Bilanin, and J. Hardin, "Bio-inspired delayed stall propulsor," *IEEE J. Ocean. Eng.*, vol. 29, no. 3, pp. 756–765, Jul. 2004.
- [60] J. Belmonte, H. Eisenberg, and E. Moses, "From flutter to tumble: Inertial drag and froude similarity in falling paper," *Phys. Rev. Lett.*, vol. 81, pp. 345–348, 1998.
- [61] Y. G. Aleyev, *Nekton*. The Hague: Dr. W. Junk Publishers, 1977.
- [62] J. J. Videler, *Fish Swimming*. London, U.K.: Chapman Hall, 1993.
- [63] F. E. Fish, "Performance constraints on the maneuverability of flexible and rigid biological systems," in *Proc. 11th Int. Symp. Unmanned Untethered Submersible Technology*. Durham, NH, 1999, pp. 394–406.
- [64] J. J. Rohr, E. W. Hendricks, L. Quigley, F. E. Fish, J. W. Gilpatrick, and J. Scardina-Ludwig, "Observations of dolphin swimming speed and strouhal number," U.S. Navy Space and Naval Warfare Systems Center, San Diego, CA, Tech. Rep. 1769, 1998.
- [65] P. R. Bandyopadhyay, J. M. Castano, W. H. Nedderman, and M. J. Donnelly, "Experimental simulation of fish-inspired unsteady vortex dynamics on a rigid cylinder," *ASME J. Fluids Eng.*, vol. 122, no. 2, pp. 219–238, 2000.
- [66] T. G. Lang and D. A. Daybell, "Porpoise performance tests in a seawater tank," Naval Ordnance Test Station Tech. Rep. 3063, 1963.
- [67] F. Fish, "Power output and propulsive efficiency of swimming bottlenose dolphins (*tursiops truncatus*)," *J. Exp. Biol.*, vol. 185, pp. 179–193, 1993.
- [68] M. Kayan and V. Y. Pyatetskiy, "Kinematics of bottlenosed dolphins swimming as related to acceleration mode," *Bionika*, vol. 11, pp. 36–41, 1977.
- [69] S. G. Lekoudis, "Computational fluid dynamics—Navy perspective," *ONR Newsletter*, vol. 3, no. 1, pp. 1–4, 1994.
- [70] A. Azuma, *The Bio-Kinetics of Flying and Swimming*. New York: Springer-Verlag, 1992.
- [71] J. J. Rohr, F. E. Fish, and J. W. Gilpatrick, "Maximum swim speeds of captive and free-ranging delphinids: critical analysis of extraordinary performance," *Marine Mammal Sci.*, vol. 18, no. 1, pp. 1–19, 2002.
- [72] S. F. Hoerner, *Fluid Dynamic Drag*. Albuquerque, NM: Hoerner, 1965.
- [73] J. R. Hunter and J. R. Zweifel, "Swimming speed, tail beat frequency, tail beat amplitude, and size in mackerel *trachurus declivis* and other fishes," *Fishery Bull.*, vol. 69, pp. 253–266, 1971.
- [74] V. Y. Pyatetskiy, "Kinematic swimming characteristics of some fast marine fish," *Bionika*, vol. 4, pp. 11–20, 1970.
- [75] R. Bainbridge, "The speed of swimming of fish as related to size and the frequency and amplitude of the tail beat," *J. Exp. Biol.*, vol. 35, pp. 109–133, 1958.
- [76] ———, "Speed and stamina of three fishes," *J. Exp. Biol.*, vol. 37, pp. 129–153, 1960.
- [77] P. W. Webb, "Effects of partial caudal-fin amputation on the kinematics and metabolic rate of under-yearling sockeye salmon (*oncorhynchus nerka*) at steady swimming speed," *J. Exp. Biol.*, vol. 59, pp. 565–581, 1973.
- [78] ———, "The swimming energetics of trout: Thrust and power output at cruise speeds," *J. Exp. Biol.*, vol. 55, pp. 489–520, 1971.
- [79] G. T. Yates, "Hydromechanics of body and caudal fin propulsion," in *Fish Biomechanics*, P. W. Webb and D. Weihs, Eds. New York: Praeger, 1983.
- [80] M. Kramer, "Hydrodynamics of the dolphin," in *Advances in Hydroscience*, V. T. Chow, Ed. New York: Academic, 1965, vol. 2, pp. 111–130.
- [81] C. S. Wardle, "Limit of fish swimming speed," *Nature*, vol. 255, pp. 725–727, 1975.
- [82] J. A. Walker, private communication, 2002.
- [83] ———, "Does rigid body limit maneuverability?," *J. Exp. Biol.*, vol. 203, pp. 3391–3396, 2000.
- [84] C. L. Gerstner, "Maneuverability of four species of coral-reef fish that differ in body and pectoral-fin morphology," *Can. J. Zool.*, vol. 77, pp. 1102–1110, 1999.
- [85] P. W. Webb and A. G. Fairchild, "Performance and maneuverability of three species of teleostean fishes," *Can. J. Zool.*, vol. 79, pp. 1866–1877, 2001.
- [86] F. E. Fish and J. Rohr, "Review of dolphin hydrodynamics and swimming performance," San Diego, CA, SPAWAR System Center Tech. Rep. 1801, 1999.
- [87] I. K. Bartol, M. S. Gordon, M. Gharib, J. R. Hove, P. W. Webb, and D. Weihs, "Flow pattern around the carapaces of rigid-bodied, multi-propulsor boxfishes (*teleostei: ostraciidae*)," *Integ. Comp. Biol.*, vol. 42, pp. 971–980, 2002.

- [88] S. D. Wilga and G. V. Lauder, "Locomotion in sturgeon: function of the pectoral fins," *J. Exp. Biol.*, vol. 202, pp. 2413–2432, 1999.
- [89] M. H. Dickinson, private communication, 2002.
- [90] A. E. Minetti and L. P. Ardigo, "Halteres used in ancient olympic long jump," *Nature*, vol. 420, no. 14, pp. 141–142, 2002.
- [91] Z. J. Wang, "Vortex shedding and optimal flapping flight," *J. Fluid Mech.*, vol. 410, p. 323, 2000.
- [92] ———, "Two-dimensional mechanism for insect hovering," *Phys. Rev. Lett.*, vol. 85, no. 10, p. 2035, 2000.
- [93] C. P. Ellington, C. v. d. Berg, A. P. Willmott, and A. L. R. Thomas, "Leading-edge vortices in insect flight," *Nature*, vol. 384, pp. 626–630, 1996.
- [94] C. P. Ellington, "The aerodynamics of hovering insect flight, IV. Aerodynamic mechanisms," *Phil. Trans. R. Soc., ser. B* 305, pp. 79–113, 1984.
- [95] T. Weis-Fogh, "Quick estimates of flight fitness in hovering animals, including novel mechanisms for lift production," *J. Exp. Biol.*, vol. 59, pp. 169–230, 1973.
- [96] G. Lauder, private communication, 2002.
- [97] A. B. Gibb, C. Jayne, and G. V. Lauder, "Kinematics of pectoral fin locomotion in the bluegill sunfish *lepisomis macrochirus*," *J. Exp. Biol.*, vol. 189, pp. 133–161, 1994.
- [98] E. G. Drucker and G. V. Lauder, "Locomotor forces on a swimming fish: Three-dimensional vortex wake dynamics quantified using digital particle image velocimetry," *J. Exp. Biol.*, vol. 202, pp. 2393–2412, 1999.
- [99] ———, "A hydrodynamic analysis of fish swimming speed: Wake structure and locomotor force in slow and fast labriform swimmers," *J. Exp. Biol.*, vol. 203, pp. 2379–2393, 2000.
- [100] ———, "Wake dynamics and fluid forces of turning maneuvers in sunfish," *J. Exp. Biol.*, vol. 204, pp. 431–442, 2001.
- [101] ———, "Locomotor function of the dorsal fin in teleost fishes: Experimental analysis of wake forces in sunfish," *J. Exp. Biol.*, vol. 204, pp. 2943–2958, 2001.
- [102] ———, "Function of pectoral fins in rainbow trout: behavioral repertoire and hydrodynamic forces," *J. Exp. Biol.*, vol. 206, pp. 813–826, 2003.
- [103] A. Gongwer, "1960s Man Powered 'AQUEON,'" U.S. Patents 3 122759 (filed 2/10/61, issued 3/3/64); 3 204 262 (filed 2/10/61, issued 9/7/65); and 3 204 699 (filed 2/10/61, issued 9/7/65).
- [104] R. Taggart, *Marine Propulsion: Principles and Evolution*. Houston, TX: Gulf, 1969.
- [105] M. Wilson, *Proc. Office of Naval Research Pre-Workshop on High-Lift Biorobotics*, P. R. Bandyopadhyay, R. Gisiner, and H. Bright, Eds., Arlington, VA, Jan. 29, 2002.
- [106] J. O. Scherer, "Experimental and theoretical investigation of large amplitude oscillating foil propulsion systems," Hydronautics, Inc., Tech. Rep. 662-1, May 1968.
- [107] S. Sandberg, R. Ramamurti, R. Lohner, J. A. Walker, and M. M. Westneat, "Pectoral fin flapping with and without deformations in the bird wrasse: 3-D unsteady computations," *J. Exp. Biol.*, vol. 205, pp. 2997–3008, 2002.
- [108] M. W. Westneat, "Functional morphology of aquatic flight in fishes: kinematics, electromyography, and mechanical modeling of labriform locomotion," *Am. Zool.*, vol. 36, pp. 582–598, 1996.
- [109] U. Piomelli, "Large-eddy simulation: achievements and challenges," *Prog. Aerospace Sci.*, vol. 35, pp. 335–362, 1997.
- [110] K. D. Squires, J. R. Forsythe, S. A. Morton, W. Z. Strang, K. E. Wurtzler, R. F. Tomaro, M. J. Grismer, and P. R. Spalart, "Progress on detached-eddy simulation of massively separated flows," Aerospace Sciences Meeting, Reno, NV, AIAA Paper 2002-1021, Jan. 2002.
- [111] C. S. Peskin, "Numerical analysis of blood flow in the heart," *J. Comput. Phys.*, vol. 25, pp. 229–252, 1977.
- [112] M. S. Triantafyllou, private communication, 2002.
- [113] A. Voet, J. G. Voet, and C. W. Pratt, *Fundamentals of Biochemistry*. New York: Wiley, 2002.
- [114] L. C. Rome, "Testing a muscle's design," *Amer. Scientist*, vol. 85, pp. 356–363, 1997.
- [115] Q. Zhang, private communication, 2003.
- [116] I. Hunter and J. Madden, private communication, 2002.
- [117] P. G. Madden, J. D. Madden, P. A. Anquetil, H. Yu, T. M. Swager, and I. W. Hunter, "Conducting polymers as building blocks for biomimetic systems," in *Proc. 12th Int. Symp. Unmanned Untethered Submersible Technology (UUST01)*. Lee, NH, Aug. 27–29, 2001.
- [118] R. H. Baughman, C. Cui, A. A. Zakhidov, Z. Iqbal, J. N. Barisci, G. M. Spinks, G. G. Wallace, A. Mazzoldi, D. D. Rossi, A. G. Rinzler, O. Jaschinski, S. Roth, and M. Kertesz, "Carbon nanotube actuators," *Science*, vol. 284, pp. 1340–1344, 1999.
- [119] (2002) DARPA CBS-ONR-ARL U.S. Navy Marine Mammal Program. Biosonar Program Office, SPAWAR Systems Center, San Diego, CA. [Online]. Available: <http://www.sparawar.navy.mil/sandiego/technology/mammals/research.html>
- [120] R. J. Full, "Invertebrate locomotor systems," in *The Handbook of Comparative Physiology*, W. Dantzler, Ed. Oxford, U.K.: Oxford Univ. Press, 1997, pp. 853–930.
- [121] R. J. Full and K. Meijer, "Metrics of natural muscle function," in *Electro Active Polymers (EAP) as Artificial Muscles, Reality Potential and Challenges*, Y. Bar-Cohen, Ed. Bellingham, WA: SPIE William Andrew/Noyes, 2001, pp. 67–83.
- [122] R. H. Baughman, L. W. Shacklette, R. L. Elsenbaumer, E. J. Plichta, and C. Bech, *Conjugated Polymeric Materials: Opportunities in Electronics, Optoelectronics, and Molecular Electronics*, J. L. Bredas and R. R. Chance, Eds. Dordrecht, The Netherlands: Kluwer, 1990, vol. 182, pp. 559–582.
- [123] R. H. Baughman, "Conducting polymer artificial muscles," *Synth. Met.*, vol. 78, pp. 339–353, 1996.
- [124] J. D. Madden, P. G. Madden, and I. W. Hunter, *Proc. SPIE 8th Annu. Symp. Smart Structures and Materials: Electroactive Polymer Actuators and Devices*, Y. Bar-Cohen, Ed. Bellingham, WA: SPIE, 2001.
- [125] Y. Bar-Cohen, *Electroactive Polymer Actuators as Artificial Muscles: Reality, Potential and Challenges*. Bellingham, WA: SPIE, 2001.
- [126] J. A. Spudich, "How molecular motors work," *Nature*, vol. 372, p. 515, 1994.
- [127] P. R. Bandyopadhyay, W. P. Krol, D. P. Thivierge, W. H. Nedderman, and M. Mojarrad, "A Biomimetic Propulsor for Active Noise Control: Experiments," Naval Undersea Warfare Center, Newport, RI, Tech. Rep. 11,351, March 2002.
- [128] P. R. Bandyopadhyay, "Emerging approaches to flow control in hydrodynamics," in *Proc. 38th IEEE Conf. Decision and Control*, Tempe, AZ, Dec. 7–10, 1999, CDC99-INVOI34, pp. 2845–2850.
- [129] V. Patricio, K. Morgansen, and J. Burdick, "Underwater locomotion from oscillatory shape deformation," in *Proc. IEEE Conf. Decision and Control*, Las Vegas, NV, Dec. 2002, pp. 2074–2080.
- [130] S. Vogel, *Life in Moving Fluids: The Physical Biology of Flows*, 2nd ed. Princeton, NJ: Princeton Univ. Press, 1994.
- [131] F. E. Fish, "Review of natural underwater modes of propulsion," DARPA, 2000.
- [132] M. W. Westneat and J. A. Walker, "Motor patterns of labriform locomotion: Kinematic and electromyographic analysis of pectoral fin swimming in the labrid fish *gomphosus varius*," *J. Exp. Biol.*, vol. 200, pp. 1881–1893, 1997.
- [133] J. A. Walker and M. W. Westneat, "Mechanical performance of aquatic rowing and flying," *Proc. Roy. Soc. Lond. B*, vol. 267, pp. 1875–1881, 2000.
- [134] M. W. Westneat and S. W. Wainwright, "Mechanical design for swimming: Muscle, tendon, and bone," *Fish Physiol. Tuna.*, vol. 19, pp. 271–311, 2001.
- [135] W. P. Chan, F. Prete, and M. H. Dickinson, "Visual input to the efferent control system of a fly's 'gyroscope,'" *Science*, vol. 280, pp. 289–292, 1998.
- [136] D. A. Pabst, "Springs in swimming animals," *Am. Zool.*, vol. 36, pp. 723–735, 1996.
- [137] F. A. Mussa-Ivaldi, S. F. Giszter, and E. Bizzi, "Motor space coding in the central nervous system," in *Cold Spring Harbor Symp. Quant. Biol.*, vol. 55, 1990, pp. 827–835.
- [138] ———, "Linear combination of primitives in vertebrate motor control," *Proc. Natl. Acad. Sci.*, vol. 91, pp. 7534–7538, 1994.
- [139] F. Mussa-Ivaldi, private communication, 2002.
- [140] M. Kemp, B. Hobson, J. Janet, C. Pell, and E. Tytell, "Assessing the performance of oscillating fin thruster vehicles," in *Proc. 12th Int. Symp. Unmanned Untethered Submersible Technology (UUST01)*. Lee, NH, Aug. 27–29, 2001.
- [141] S. Sandberg and R. Ramamurti, private communication, 2002.
- [142] T. Gieseke, D. Hrubes, A. Yandell, J. Walker, and N. Kato, "Pectoral fin motions for vehicle control," in *Proc. 13th Int. Symp. Unmanned Untethered Submersible Technology*, Aug. 24–27, 2003.
- [143] N. Kato, H. Liu, and H. Morikawa, "Biology-inspired precision maneuvering of underwater vehicles," in *Proc. 12th Int. Symp. Unmanned Untethered Submersible Technology (UUST01)*. Lee, NH, Aug. 27–29, 2001.
- [144] N. Kato, private communication, 2002.
- [145] W. P. Krol, A. Annaswamy, and P. W. Bandyopadhyay, "A biomimetic propulsor for active noise control," Naval Undersea Warfare Center, Newport, RI, Tech. Rep. 11,350, Feb. 2002.

- [146] O. Kreisher, "The littoral navy: SEALS, dolphins and other marine mammals," *Sea Power*, vol. 45, no. 7, pp. 49–51, 2002.
- [147] R. Bannasch, "New wing and propeller constructions inspired by techniques learned from wing-propelled animals," presented at the 1st Int. Symp. Aqua Bio-Mechanisms ISABMEC 2000, Honolulu, HI.
- [148] J. E. Haun and P. E. Nachtigall, "Artificial intelligence and bionics workshop report," Naval Oceans Systems Center, San Diego, CA, Tech. Rep., 1003, Nov. 1985.
- [149] B. D. Reger, K. M. Fleming, V. Sanguineti, S. Alford, and F. A. Mussa-Ivaldi, "Connecting brains to robots: The development of a hybrid system for the study of learning in neural tissue," *Art. Life*, vol. 6, pp. 307–324, 2000.
- [150] J. Vreeken, Spiking Neural Networks: An Introduction, Artificial Intelligence laboratory, Intelligent Systems Group, Univ. Utrecht, 2003.
- [151] H. Yu and T. M. Swager, "Molecular actuators—Designing actuating materials at the molecular level," *IEEE J. Ocean. Eng.*, vol. 29, no. 3, pp. 692–695, Jul. 2004.
- [152] S. N. Singh, A. Simha, and R. Mittal, "Biorobotic AUV maneuvering by pectoral fins: Inverse control design based on CFD optimization," *IEEE J. Ocean. Eng.*, vol. 29, no. 3, pp. 777–785, Jul. 2004.
- [153] P. R. Bandyopadhyay, "Guest editorial: Biology-inspired science and technology for autonomous underwater vehicles," *IEEE J. Ocean. Eng.*, vol. 29, no. 3, pp. 542–546, Jul. 2004.
- [154] D. Beal, P. R. Bandyopadhyay, T. Fulton, W. Krol, and A. Menozzi, "Hovering underwater: Toward a comparison of steady-state and unsteady hydrodynamics," *Bull. Amer. Phys. Soc.*, vol. 49, no. 9, p. 165, 2004.
- [155] D. Beal and P. R. Bandyopadhyay, "Toward a comparison of steady-state and unsteady hydrodynamic mechanisms," in *Proc. 14th Int. Symp. Unmanned Untethered Submersible Technology*. Lee, NH, Aug. 21–24, 2005.
- [156] M. Kemp, B. Hobson, and C. Pell, "Energetics of the oscillating fin thruster," in *Proc. 13th Int. Symp. Unmanned Untethered Submersible Technology*. Lee, NH, Aug. 24–27, 2003.



**Promode R. Bandyopadhyay** received the B.S. degree in mechanical engineering from the University of North Bengal, India, the M.S. degree from the University of Calcutta, Calcutta, India, and Ph.D. degrees from the Indian Institute of Technology, Madras, and the University of Cambridge, Cambridge, U.K., in 1968, 1970, 1974, and 1978, respectively.

He managed the ONR Biorobotics Program during 2001–2003. During that time, he built a new direction of the program with multidisciplinary investigators and an applied emphasis. He is currently with the

Naval Undersea Warfare Center, Newport, RI, where he carries out research on technologies for biology-inspired autonomy and turbulence control. His work led to the quantification of the gap in maneuverability between fish and tactical scale undersea vehicles. He also led the NUWC-Russia-U.K. compliant coating research project. While at NASA Langley Research Center earlier as an in-house contractor, he designed a stepped axisymmetric nose employing the convex curvature concept of viscous drag reduction, which has been found to have evolved in certain aquatic animals. There, he also described experimentally the regeneration mechanism of turbulent trailing vortex, which has since been confirmed by direct numerical simulation. His rough wall turbulent boundary layer data has been used widely for code validation. While at Cambridge, via a simple experiment he, with M. R. Head, elucidated the inclined organized hairpin vortex structure of turbulent boundary layers and the thinning effect of increasing Reynolds number on them which have been subsequently confirmed by numerous simulations and experiments. He was an Adjunct Faculty Member at ODU and URI.

Dr. Bandyopadhyay is a Fellow of ASME and Wolfson College at the University of Cambridge. He has received the NASA Award for Technology Utilization and Application for a skin friction meter. Four of his works are cited in twelve text books. He was the Founding Editor of the ASME volume on the *Application of Microfabrication to Fluid Mechanics*. He has served as Associate Editor of the *AIAA Journal* and the *ASME Journal of Fluids Engineering*, and as the Guest Editor of the Special Issue on Biology-Inspired Science and Technology for Autonomous Undersea Vehicles of the *IEEE JOURNAL OF OCEANIC ENGINEERING*.